



HAL
open science

Electronic Effects in Phosphino-Iminophosphorane Pd II Complexes upon Varying the N Substituent

Ingrid Popovici, Elise Lognon, Nicolas Casaretto, Antonio Monari, Audrey Auffrant

► To cite this version:

Ingrid Popovici, Elise Lognon, Nicolas Casaretto, Antonio Monari, Audrey Auffrant. Electronic Effects in Phosphino-Iminophosphorane Pd II Complexes upon Varying the N Substituent. *Chemistry - A European Journal*, 2023, 30 (5), 10.1002/chem.202303350 . hal-04772171

HAL Id: hal-04772171

<https://hal.science/hal-04772171v1>

Submitted on 19 Nov 2024

HAL is a multi-disciplinary open access archive for the deposit and dissemination of scientific research documents, whether they are published or not. The documents may come from teaching and research institutions in France or abroad, or from public or private research centers.

L'archive ouverte pluridisciplinaire **HAL**, est destinée au dépôt et à la diffusion de documents scientifiques de niveau recherche, publiés ou non, émanant des établissements d'enseignement et de recherche français ou étrangers, des laboratoires publics ou privés.

Electronic effects in Phosphino-Iminophosphorane Pd^{II} complexes upon varying the N substituent

Ingrid Popovici,^[a] Elise Lognon,^[b] Nicolas Casaretto,^[a] Antonio Monari,^{*[b]} and Audrey Auffrant^{*[a]}

[a] I. Popovici, Dr. N. Casaretto, Dr. A. Auffrant
Laboratoire de Chimie Moléculaire (LCM),
CNRS, École Polytechnique, Institut Polytechnique de Paris
Route de Saclay,
91120 Palaiseau, France.
E-mail: audrey.auffrant@polytechnique.edu

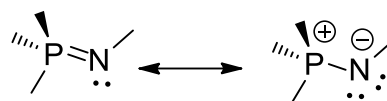
[b] Dr. E. Lognon, Dr. A. Monari
ITODYS
Université Paris Cité and CNRS
F-75006, Paris, France.
E-mail: antonio.monari@u-paris.fr

Abstract: Three series of palladium(II) complexes supported by a phosphine-iminophosphorane ligand built upon an ortho-phenylene core were investigated to study the influence of the N substituent. *Cis*-dichloride palladium(II) complexes **1** in which the N atom bears an isopropyl (iPr, **1a**), a phenyl (Ph, **1b**), a trimethylsilyl (TMS, **1c**) group or an H atom (**1d**) were synthesized in high yield. They were characterized by multinuclear NMR, IR spectroscopy, HR-mass spectrometry, and X-ray diffraction. A substantial bond length difference between the Pd-Cl bonds was observed in **1**. Complexes **1a-d** were converted in [Pd(L^R)Cl(CN^tBu)](OTf) **2a-d** in which the isocyanide is located *trans* to the iminophosphorane. The corresponding dicationic complexes [Pd(L^R)(CN^tBu)₂](OTf)₂ **3a-d** were also synthesized, however they exhibited compared to **2** a much decreased stability in solution, the isopropyl derivative **3a** being the most stable of the series. Molecular modelling was performed to rationalize the regioselectivity of the chloride by isocyanide monosubstitution (from **1** to **2**) and to study the electronic distribution in the different complexes. In particular differences between the TMS and H containing complexes vs the iPr and Ph ones were found. This suggests that the nature of the N substituent is far from innocent and can help tune the reactivity of iminophosphorane complexes.

Introduction

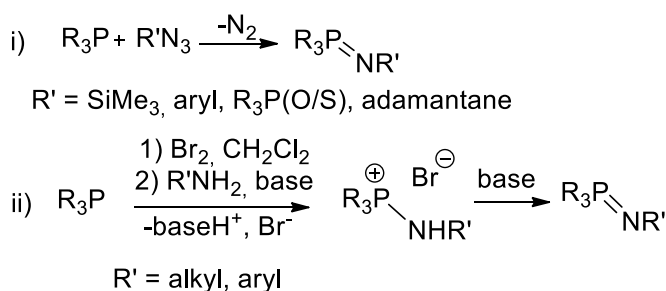
Iminophosphoranes or phosphinimines were discovered in 1919 by Staudinger and Meyer when they oxidized phosphines with azides,^[1] a transformation now known as the Staudinger reaction. Nowadays these PR₃=NR' derivatives have found numerous applications in (bio)organic chemistry^[2] or as organocatalysts^[3] thanks to their strong basicity.^[4] In such ylidic compounds the electron density is localized on the nitrogen that features two lone pairs, which are stabilized by the electron-deficient phosphorus atom. Even if iminophosphoranes are always represented with a double bond to underline the strong interaction between the phosphorus and the nitrogen atoms, there is no π system in these compounds. The stabilization by the phosphorus is due to

negative hyperconjugation explaining that the P-N bond is shorter than a single one and that P-C bonds are elongated compared to the corresponding phosphines.^[5] Therefore, they are best described as a resonance hybrid of two limit forms the ylene and the ylidic ones (Scheme 1).



Scheme 1: Lewis representation of the two limit forms of iminophosphoranes

Their use in coordination chemistry started in the sixties with monodentate ligands.^[6] In line with their electronic properties they were found quite labile on electron rich metals,^[7] and were incorporated in polydentate structures.^[6, 8] Iminophosphoranes behave as strong σ and π donors that do not exhibit accepting ability which explain that, contrary to imines, they are not reduced in presence of low-valent metals.^[9] Even if they remain largely less investigated than their carbon congeners, their potential in transition-metal catalyzed reactions has also been investigated.^[6, 8b, 10] Early this year, we were interested in comparing the electronic properties of phosphonium ylides and iminophosphorane focusing on square planar dicarbonyl complexes featuring a mixed phosphine-ylide ligand built on a rigid ortho-phenylene skeleton. We showed that the nitrogen substituent in the iminophosphorane group influenced the electronic property of the ligand. In this study the isopropyl substituent helped the P=N group competing in terms of electron donation with the P⁺-CH₂⁻ containing ligand.^[11]



Scheme 2. Synthetic access to the P=N linkage

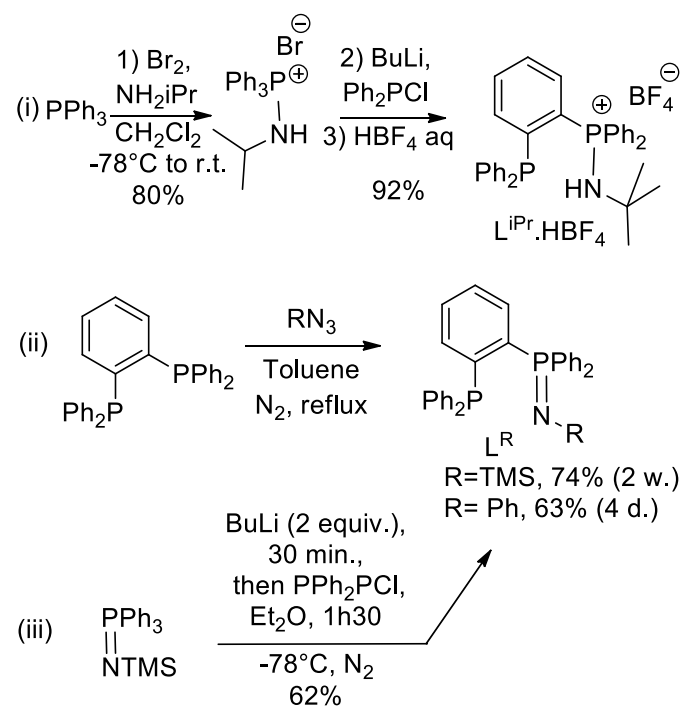
Nevertheless, this influence has not been previously investigated because the nature of the substituent is generally dictated by the way the P=N linkage is formed. Indeed, the Staudinger reaction is generally conducted with stable azides which feature a trimethylsilyl, a (thio)phosphonate, a bulky adamantane, or an aryl group (Scheme 2i). Small alkyl substituted nitrogen atom containing iminophosphoranes are accessible thanks to the modified Kirsanov reaction^[12] when employing light primary amines (Scheme 2ii). The latter generally leads to aminophosphoniums, i.e the conjugated acids of the iminophosphoranes. With the aim to investigate the influence of the nitrogen substituent on the electron donating properties of the ligand and consequently in the reactivity/stability of the complexes we have synthesized three series of Pd^{II} complexes supported by a mixed phosphine-iminophosphorane ligand built on the rigid ortho-phenylene scaffold, where the N substituent is an isopropyl (iPr, **1a**), a phenyl (Ph, **1b**), a trimethylsilyl (TMS, **1c**) group or an H atom (**1d**). Starting from the dichloride palladium(II) complexes (series **1**) we introduced one (series **2**) and two (series **3**) isocyanide ligands to serve as IR probes. The experimental results were completed by molecular modeling and are presented and discussed in the following.

Results and Discussion

Synthesis and characterization of L^R supported Pd^{II} complexes

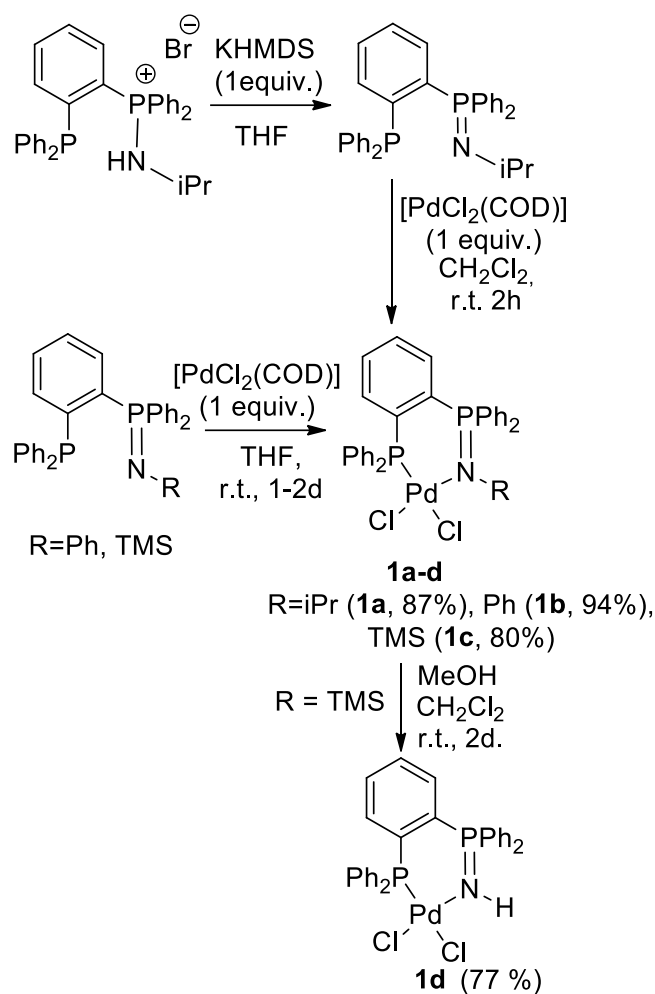
Given our objective to quantify the influence of the nitrogen substituent on the electron donating properties of the iminophosphorane function, four different phosphine-iminophosphorane/aminophosphonium derivatives have been synthesized (Scheme 3). L^{iPr}.HBF₄ was prepared as previously published via a 2- step procedure from PPh₃.^[13] To prepare L^{Ph}, the 1,2-bis(diphenylphosphino)benzene was reacted with one equivalent of phenylazide and the iminophosphorane was isolated by precipitation from toluene in 63% yield (Scheme 2ii). Its crystal structure is presented in Figure S1. Compared to the parameters reported for PPh₃=NPh,^[5b] the PN bond is shorter while the N-C_{Ph} is longer, and the angular parameters are very similar. The preparation of L^{TMS} was first attempted, as previously described,^[14] via a Staudinger reaction between trimethylsilylazide and the disphosphine in toluene at reflux. In our hands, the reaction lasted 2 weeks. Therefore, L^{TMS} was

alternatively prepared by the ortholithiation of PPh₃=NTMS^[15] and reaction with diphenylphosphinechloride (Scheme 2iii) giving the expected ligand in 62% yield.



Scheme 3: Synthesis of the (pro)ligands.

The preparation of L^H by desilylation of L^{TMS} in methanol was attempted but the formed compound could not be isolated.^[14b] So, the desilylation was conducted after the metalation (vide infra). The palladium dichloride complexes **1** were formed by reacting the phosphine-iminophosphorane ligand with [PdCl₂(COD)]^[16] at room temperature (Scheme 4). For R=iPr, the coordination was preceded by a deprotonation which was done in THF with one equivalent hexamethyldisilazane (KHMDs). In-situ ³¹P{¹H} NMR monitoring ascertained the complete formation of the L^{iPr} ligand characterized by a doublet at δ_P = -1.18 and -13.67 (J_{P,P} = 13.0 Hz) in THF. After filtration to remove the potassium salt, THF was replaced by CH₂Cl₂, and the addition of the Pd precursor cleanly formed [Pd(L^{iPr})Cl₂] (**1a**) within 2 h at room temperature. It was isolated as a bright yellow solid in 87% yield by precipitation upon concentration of the reaction mixture. The coordination of L^{Ph} and L^{TMS} were carried out with the same precursor in THF, the complexes [Pd(L^R)Cl₂] **1b** (R= Ph) and **1c** (R= TMS) were isolated in respectively 94% and 80% yield. [Pd(L^H)Cl₂] (**1d**) was formed by methanolysis of **1c** (Scheme 4). The latter precipitated from the reaction mixture together with grey particles, being probably Pd⁰. The reaction was followed by *in situ* ³¹P NMR and stopped when the starting material had disappeared. After purification, **1d** was isolated in 77% yield as a light-yellow solid.



Scheme 4: Synthesis of $[\text{Pd}(\text{L}^{\text{R}})\text{Cl}_2]$ **1** complexes

These complexes were characterized by multinuclear NMR spectroscopy (^{31}P , ^1H , ^{13}C), HR-mass spectrometry, elemental analysis, and X-ray crystallography. Their ^{31}P NMR spectrum exhibited 2 doublets at 11.9, 22.4 ppm for **1a**, 11.9, 23.5 ppm for **1b**, 15.8, 20.5 ppm for **1c**, and 17.7, 32.0 ppm for **1d**. The nature of the N-substituent has only a little influence on the measured chemical shifts nevertheless for the **1d** both signals are deshielded. Their ^1H and ^{13}C NMR spectra are highly similar and mostly differ by the signals corresponding to the N-substituents. Note that the resonance of the NH proton for **1d** could not be observed.

Single crystals of these complexes were grown by diffusion of pentane vapors into dichloromethane solution of the compounds. The obtained structures are presented in Figure 2 together with selected metrics and angles. All the complexes are square planar as expected with only a small deviation to planarity (see table S4). Moreover, the metrics and angles for complexes **1a-d** are globally very similar, in particular the Pd-N and the P=N bonds do not experience significant variations upon modifying the N substituent. Yet, a substantial dissymmetry in the Pd-Cl bond lengths was observed for these complexes **1**; the chloride *trans* to the iminophosphorane is slightly closer to the Pd than the *cis* one. As

the iminophosphorane is a harder donor than the phosphine group, a stronger *trans* influence of the former,^[17] and thus an opposite trend, may have been expected. The observed relative bond length order may be reminiscent of the inverse *trans* influence which was previously investigated within f-elements^[18] or cobalt complexes.^[19] Noteworthy, all the 16 other structures of monomeric square planar dichloride Pd^{II} complexes supported by a phosphine-iminophosphorane ligand reported in the CCDC database show a shorter Pd-Cl distance *trans* to N compared to the *cis* one.^[20] This observation on **1a-d** was further investigated by molecular modeling (vide supra).

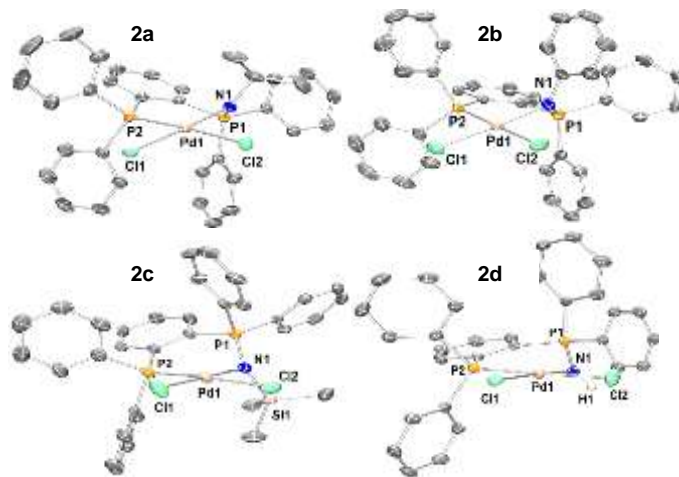
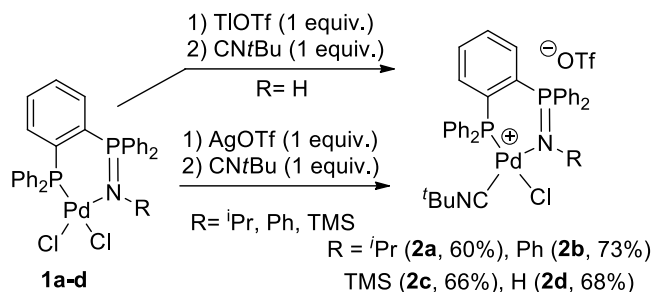


Figure 2: X-ray structure of $[\text{Pd}(\text{L}^{\text{R}})\text{Cl}_2]$ (**1a** R=iPr, **1b** R=Ph, **1c** R=TMS, **1d** R=H) with thermal ellipsoids (drawn at the 50% probability level). The H atoms and a CH_2Cl_2 molecule (for **1a**) were omitted for clarity. Selected bond lengths [Å] and angles [°]: **1a** Pd1-N1 = 2.060(2); Pd1-P2 = 2.2223(7); Pd1-Cl1 = 2.3305(7); Pd1-Cl2 = 2.3931(7); P1-N1 = 1.599(2); N1-Pd1-P2 = 94.81(7); P2-Pd1-Cl1 = 83.81(2); Cl1-Pd1-Cl2 = 91.22(2); N1-Pd1-Cl2 = 90.17(7); **1b** Pd1-N1 = 2.050(4); Pd1-P2 = 2.2222(9); Pd1-Cl1 = 2.3064(12); Pd1-Cl2 = 2.3582(9); P1-N1 = 1.590(4); N1-Pd1-P2 = 91.04(9); P2-Pd1-Cl1 = 88.43(4); Cl1-Pd1-Cl2 = 89.88(4); N1-Pd1-Cl2 = 90.46(9); **1c** Pd1-N1 = 2.079(5); Pd1-P2 = 2.2327(17); Pd1-Cl1 = 2.2970(19); Pd1-Cl2 = 2.3977(17); P1-N1 = 1.590(5); N1-Pd1-P2 = 90.67(14); P2-Pd1-Cl1 = 89.34(6); Cl1-Pd1-Cl2 = 91.84(6); N1-Pd1-Cl2 = 88.16(14); **1d** Pd1-N1 = 2.027(2); Pd1-P2 = 2.2210(8); Pd1-Cl1 = 2.3172(8); Pd1-Cl2 = 2.3659(8); P1-N1 = 1.595(2); N1-Pd1-P2 = 93.41(7); P2-Pd1-Cl1 = 86.57(3); Cl1-Pd1-Cl2 = 92.95(3); N1-Pd1-Cl2 = 87.16(7).

In order to evaluate the donation of the ligand and more precisely the impact of the N substituent on its electronic properties, one chloride was substituted by an isocyanide. The latter was chosen as a suitable IR probe to precisely control the incorporated amount, which would not be easily feasible with CO. In addition, unlike CO, isocyanide cannot enter deleterious aza-Wittig reactions which may occur in presence of an iminophosphorane. The monosubstitution reaction may lead to a mixture of two isomeric complexes, but the difference of Pd-Cl bond lengths in **1** may lead to a considerable isomeric excess.

To synthesize $[\text{Pd}(\text{L}^{\text{R}})\text{Cl}(\text{tBuCN})](\text{OTf})$ **2** complexes (Scheme 5), the dichloride complexes **1** were reacted with one equivalent of AgOTf to abstract the chloride. After the silver salt was filtered off, a solution of tertbutylisocyanide (1 equivalent) was added to the reaction mixture. The cationic complexes **2** were isolated after evaporation of the volatiles and washing with diethyl ether. This protocol allowed to synthesize **2** for R= iPr (**2a**), Ph (**2b**), and TMS (**2c**) in respectively 60, 73, and 58% yield. In each case, the

formation of a single compound identified by the presence of two doublets in $^{31}\text{P}\{^1\text{H}\}$ NMR spectroscopy was observed, confirming the selectivity of the substitution. Here again the recorded chemical shifts were very similar for **2a-c** (14.1 and 26.0 ppm for **2a**, 14.4 and 26.4 for **2b**, 19.4 and 26.6 ppm for **2c**).

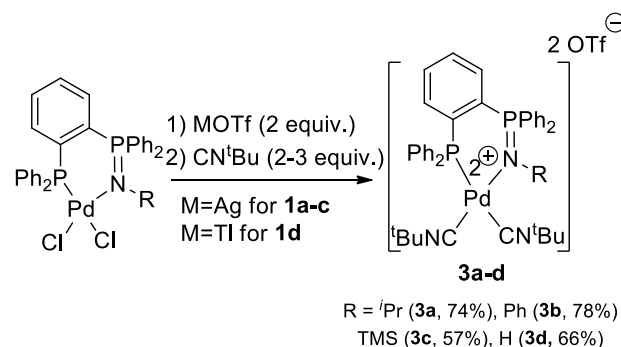


Scheme 5. Synthesis of $[\text{Pd}(\text{L}^{\text{R}})\text{Cl}(\text{tBuCN})](\text{OTf})$ **2** complexes

For **1d**, the reaction with AgOTf was not satisfying as the $^{31}\text{P}\{^1\text{H}\}$ NMR spectrum of the crude mixture showed various resonances among which some corresponding to Ag^{I} coordinated PPh_2 units, recognizable thanks to their complex coupling pattern due to the two Ag^{I} isotopes (^{107}Ag and ^{110}Ag). It was hypothesized that the lower steric hindrance at the N atom may be at the origin of this transmetalation side reaction. To circumvent this difficulty, a thallium salt, which has been successfully used for Fe^{II} iminophosphorane complexes^[21] was employed allowing to isolate $[\text{Pd}(\text{L}^{\text{H}})\text{Cl}(\text{tBuCN})](\text{OTf})$ **2d** in 68 % yield. In the series of complexes **2**, **2c** and **2d** appeared as the most sensitive, since they decomposed after some hours in dichloromethane while exchange reactions occurred in acetonitrile rendering their $^{13}\text{C}\{^1\text{H}\}$ NMR characterization difficult. The higher sensitivity of **2d** could be due to the lower steric hindrance at the N atom, for **2c** it may be explained by electronic effects. This will be further discussed with molecular modeling (vide infra). Complexes **2** were also characterized by elemental analysis, HR-mass spectrometry, IR spectroscopy and X-ray diffraction analysis. The IR $\text{C}\equiv\text{N}$ stretching frequencies of complexes **2a-d** were observed at 2227, 2234, 2229, and 2228 cm^{-1} respectively (Table S6). Even if these frequencies are very close they increase in the series $\text{iPr} > \text{H} > \text{TMS} > \text{Ph}$, which may suggest a stronger backdonation and therefore a weaker CN bond in the case of **2a**.

Single crystals were obtained by gas diffusion of diethyl ether into concentrated dichloromethane solution of the complex. The latter are presented in Figure 3 together with selected bond lengths and angles. For **2c**, only a low-quality structure was obtained despite numerous attempts. All these mono isocyanide complexes exhibit a square planar geometry and the isocyanide ligand is consistently localized *trans* to the iminophosphorane group. As a consequence, the substitution of the chloride exhibiting the shortest Pd-Cl bond in the series of complexes **2** has occurred preferentially. This result may appear rather astonishing because generally a shorter interatomic distance is associated to a stronger bond and therefore a less reactive and worse leaving

group. This rather counter intuitive observation has been further investigated computationally (vide infra). As in complexes **1a-d**, the bond lengths in the first coordination sphere are rather similar in complexes **2a-d**. When comparing complexes **2a, b, d**, (**2c** was excluded from the comparison because of the quality of the structure), **2a** exhibits the longer Pd-Cl bond and **2b** the shorter Pd-C (Table S5). The deviation to planarity is not correlated to the steric hindrance because **2b** exhibits a weaker deviation than **2d** (the P2N1C1C7 torsion angles being respectively $-0.8(2)^\circ$ and $-4.36(6)^\circ$, see table S5). In addition, for all the complexes, the N substituent and the P1 atom are not located on the same side of the median plane, which allows minimizing the steric hindrance. The distances between P2 and the median plane as well as that of the atom directly linked to N (C in **2a** and **2b**, Si in **2c**, and H in **2d**) evolve in the series. The shortest ones were observed for **2d** featuring the smaller substituent, while the distance of the Si (**2c**) to the median plane is the longest one in agreement with the high steric hindrance of the SiMe_3 group. As the iminophosphorane behaves as a strong electron donating ligand, a significant backdonation occurring from the metal to the isocyanide may have been expected, resulting in the elongation of C-N bond. It was difficult to evaluate this phenomenon based on the metrics because of their rather similar magnitude, even if a tendency based on the C-N bond length may suggest that the electron-donating ability increases in the sequence $\text{R} = \text{Ph} < \text{H} < \text{iPr}$. This correlated with the measured CN wavenumber, which slightly decreased from $\text{R} = \text{Ph}$ (2234 cm^{-1}), TMS (2229 cm^{-1}), H (2228 cm^{-1}) iPr (2227 cm^{-1}) but again the differences are too tiny to be very affirmative.



Scheme 6. Synthesis of $[\text{Pd}(\text{L}^{\text{R}})\text{Cl}(\text{tBuCN})_2](\text{OTf})_2$ **3** complexes

The synthesis of dicationic complexes $[\text{Pd}(\text{L}^{\text{R}})(\text{CNtBu})_2](\text{OTf})_2$ **3** was also attempted (Scheme 6). The protocol was similar to the one employed for **2**: the halogen abstraction was achieved for **1a-c** with two equivalents of AgOTf, while TlOTf was employed with **1d**. Then, after removal of the halide salt, a solution of two equivalents CNtBu in dichloromethane was added to the reaction mixture. The dicationic diisocyanide palladium complexes $[\text{Pd}(\text{L}^{\text{R}})(\text{tBuCN})_2](\text{OTf})_2$ **3** were isolated in good yields (66-78%).

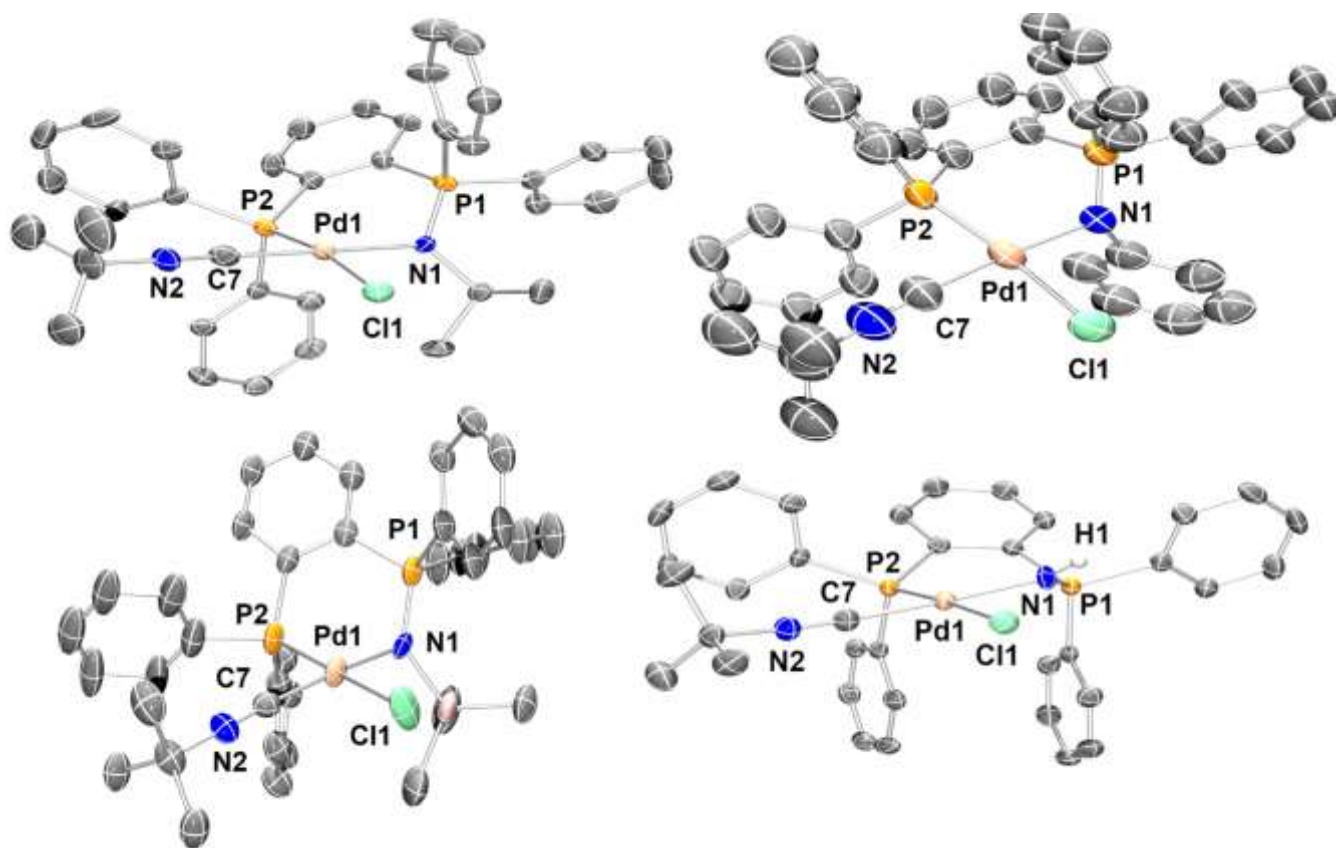


Figure 3: X-ray structure of $[\text{Pd}(\text{L}^{\text{R}})\text{Cl}(\text{BuCN})](\text{OTf})$ (**2a** R=Pr, **2b** R=Ph, **2c** R=TMS, **2d** R=H) with thermal ellipsoids (drawn at the 50% probability level). The H atoms, the triflate anion and a CH_2Cl_2 molecule (for **2a** and **2d**) were omitted. Selected bond lengths [Å] and angles [°]: **2a** Pd1-N1 = 2.069(7); Pd1-P2 = 2.240(3); Pd1-Cl1 = 2.370(2); Pd1-C7 = 1.939(11); N2-C7 = 1.149(12); P1-N1 = 1.605(7); N1-Pd1-P2 = 88.9(2); N8-Pd1-Cl1 = 95.7(2); C7-Pd1-Cl1 = 84.6(3); C7-Pd1-P2 = 91.0(3). **2b** Pd1-N1 = 2.046(7); Pd1-P2 = 2.254(3); Pd1-Cl1 = 2.338(2); Pd1-C7 = 1.919(11); N2-C7 = 1.135(12); P1-N1 = 1.590(7); N1-Pd1-P2 = 93.7(2); N2-Pd1-Cl1 = 90.4(2); C7-Pd1-Cl1 = 86.5(3); C7-Pd1-P2 = 89.4(3). **2c** Pd1-N1 = 2.05(3); Pd1-P2 = 2.197(11); Pd1-Cl1 = 2.347(11); Pd1-C7 = 1.94(3); N2-C7 = 1.17(4); P1-N1 = 1.64(3); N1-Pd1-P2 = 86.6(9); N2-Pd1-Cl1 = 95.1(9); C7-Pd1-Cl1 = 87.3(11); C7-Pd1-P2 = 91.3(11). **2d** Pd1-N1 = 2.011(2); Pd1-P2 = 2.460(6); Pd1-Cl1 = 2.3409(6); Pd1-C7 = 1.1.937(3); N2-C7 = 1.138(3); P1-N1 = 1.603(2); N1-Pd1-P2 = 94.32(6); N1-Pd1-Cl1 = 87.89(26); C7-Pd1-Cl1 = 88.31(7); C7-Pd1-P2 = 89.67(7).

Nevertheless, their limited stability in solution has precluded their complete characterization. Namely, despite numerous attempts, no single crystal suitable for X-ray diffraction could be grown. Complexes **3** were characterized by ^{31}P and ^1H NMR spectroscopy. The ^{31}P resonances were very similar, with the iminophosphorane resonating in the range 10.5-19.2 ppm and the phosphine between 29.9 and 31.3 ppm. Also, the resonance of the P=NH group in **3d** was slightly deshielded compared to those observed for complexes **3a-c**. Only **3a** (R = i Pr) could be characterized by $^{13}\text{C}\{^1\text{H}\}$ NMR, because the three others (**3b-d**) decomposed within couple of hours in acetonitrile or dichloromethane. The higher stability of **3a** may be explained by the stronger donation from L^{Pr} , while for the other complexes, a lower steric protection (L^{H}) as well as a lower electron donation (L^{Ph} , L^{TMS}) may be at the origin of the experimental observations. Only the IR spectrum of **3a** showed two bands in the isocyanide area (at 2239 and 2199 cm^{-1}), for the other complexes a rather large band was observed in this area (Table S7). Density Functional Theory (DFT) calculations were conducted in order to gain a better understanding of the differences observed in these

series of complexes and discuss the regioselectivity of the monosubstitution.

DFT modeling

The modelled complexes were labeled with Latin characters **I**, **II**, **III** corresponding to the complexes **1**, **2**, **3**. In addition *cis* and *trans* always referred to the position relative to the iminophosphorane group.

The principal bond distances obtained from molecular modeling are reported in Table 1. Coherently with the experimental results the distances were quite similar within a series of complexes. Even if the small differences observed may be sensitive to numerical and methodological errors, slight but significant tendencies can be seen among the *cis* and *trans* ligands. In particular for series **I** (Table 1) while the Pd-Cl_{*cis*} bond length averaged at 2.40 Å, the opposite one (Pd-Cl_{*trans*}) peaked at 2.36 Å. This agrees well with the experimental observations. For the series **II**, the Pd-Cl_{*cis*} bond remained rather constant and longer than the Pd-C bond (2.4 vs. 1.9 Å). Nevertheless, a slightly shorter Pd-Cl_{*cis*} bond was found for **IId**. In the series **IIIa-d** (Table 1), the general trends were respected yet a slightly less systematic behavior was observed. In particular, the Pd-C_{*cis*} bond are longer

than the *trans* ones. Regarding the CN bond lengths, no significant differences were observed.

Table 1: Bond lengths at the ground state minimum in Angstrom for modelled complexes I, II, and III. *Cis* and *trans* refer to N.

Complex	Pd-Cl _{trans}	Pd-Cl _{cis}	Pd-C _{trans}	Pd-C _{cis}	C _{trans} -N	C _{cis} -N
I	a	2.363	2.398			
	b	2.358	2.399			
	c	2.359	2.407			
	d	2.359	2.395			
II	a		2.392	1.949		1.160
	b		2.389	1.947		1.160
	c		2.398	1.949		1.161
	d		2.373	1.946		1.160
III	a			1.964	2.035	1.158
	b			1.966	2.025	1.159
	c			1.966	2.028	1.159
	d			1.966	2.016	1.159

To rationalize the formation of **2a-d** from **1a-d** the relaxed potential energy scan along the two Pd-Cl bonds for **1a-d** have been calculated (Figure 4). The potential energy surface leading to the bond dissociation for the Cl in *cis* to N was systematically swallower than the opposite one, leading to a less important energy penalty for the bond breaking. This suggests that the dissymmetry observed in the bond distances was translated onto a difference in the leaving group capacity.

Nevertheless, this does not fit with the isomer formed experimentally. With the idea that the isolated complexes **2a-d** would be the thermodynamic product of the substitution reaction, we modeled the putative triflate intermediate (**Int_{a-d}**) and the isomer presenting the isocyanide *trans* or *cis* to the iminophosphorane respectively **IIa-d** and **II'a-d** (Figure 5).

The free energy differences between the connected stationary points have been estimated with the rigid rotor approximation, thanks to the calculation of the harmonic vibrational frequencies. A stable intermediate **Int_{a-d}** exhibiting a trigonal arrangement has been positioned. It results from the loss of one ligand, while the triflate remains uncoordinated. In this intermediate the *cis/trans* dissymmetry present in the reactant **I** has been lost. The *trans* isomer product **IIa-d** was found systematically stabilized with respect to the *cis* **II'a-d** counterpart. The free energy gap between the two isomers being comprised between about 5 and 7 kcal.mol⁻¹, with **IIId** showing the larger stabilization of the *trans* isomer.

Thus, the stereoselectivity observed experimentally probably came from the thermodynamical control of the reaction. The *cis* chloride was the preferable leaving group, leading to a tricoordinated intermediate which evolved to form the more stable *trans* isomer.

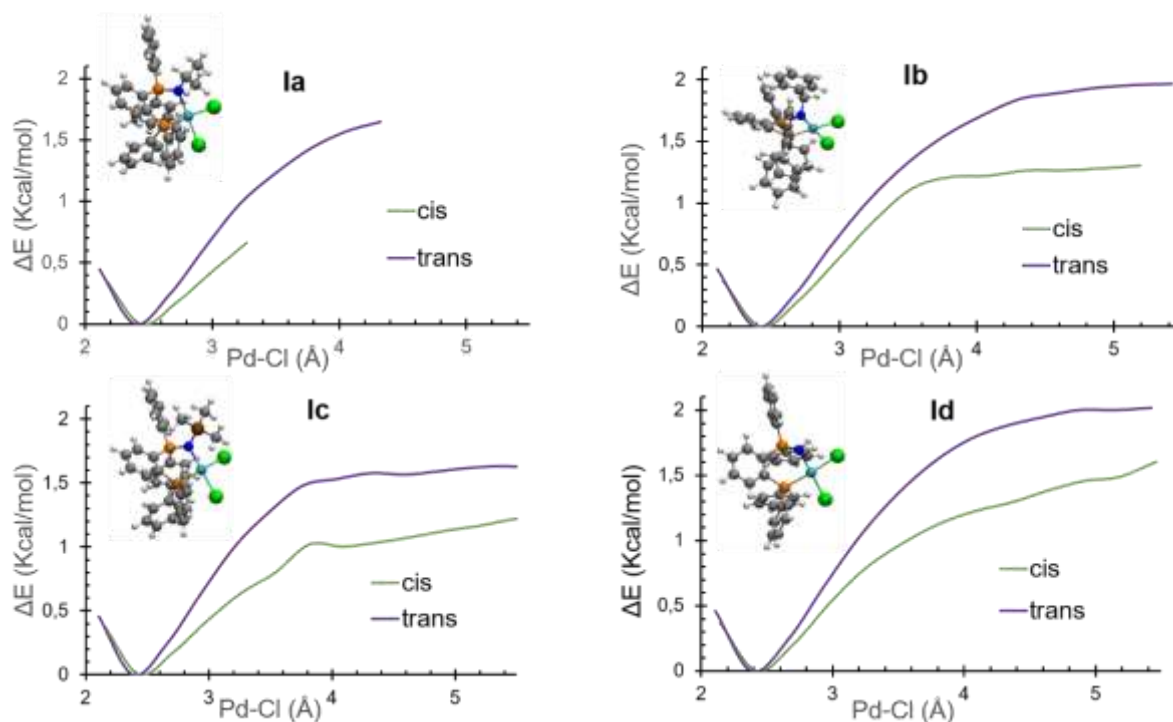


Figure 4: Elongation scan of the Pd-Cl bond for **1a-d** complexes.

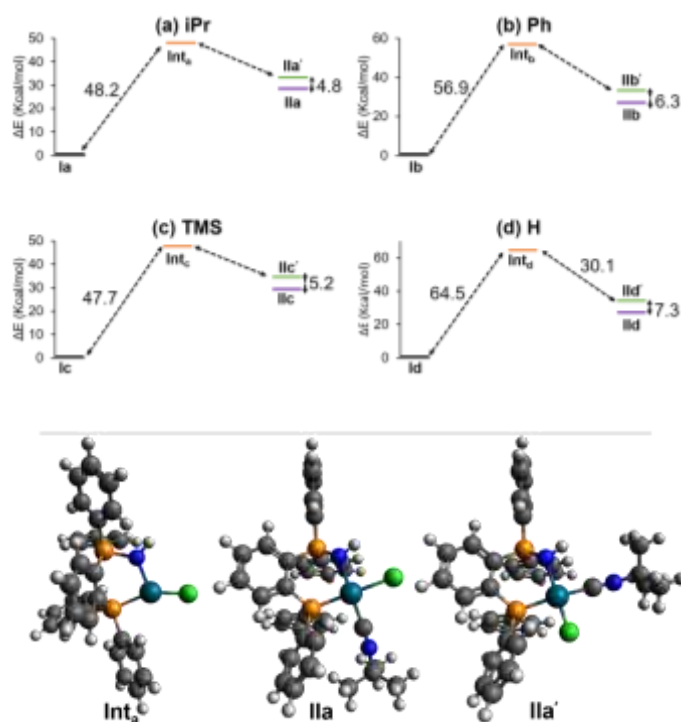


Figure 5: Scheme of difference energy in kcal.mol⁻¹ between **Ia-d** (black) as reference and the putative tricoordinated intermediate structure **Int_{a-d}** (orange). Difference energy between **Ila-d** (violet) and **Ila'-d** (green) are also reported in kcal.mol⁻¹. Optimized structures used for calculations are shown below.

Finally, to assess the peculiarity in the electronic structure properties of the complexes, we first calculated the harmonic vibrational frequencies, but as shown in Table S6-7 they didn't provide significant differences and systematic trends. This is probably due to the close values of the vibrational resonances and the use of the harmonic approximation, but it also corroborates the very close values obtained experimentally. Atomic charges for the most important atoms were then calculated (Tables 2-4) d. For modeled complexes **Ia-d**, the charge on Pd was similar with the only exception of that of **Ia** calculated at 0.16 a.u. Regarding the charge on the N atom, **Ic** exhibited the more negative one. Conversely, the charges on the other atoms experienced less pronounced variations. Interestingly, a marked difference was observed for the charges on the Cl ligands, with the chloride *trans* to the nitrogen being systematically less negative than its *cis* counterpart, which in turn showed a longer bond and a better leaving group ability.

Table 2: Principal NPA charges for complexes **Ia-d**. *Cis* and *trans* refer to N.

Complex	Ia	Ib	Ic	Id
Pd	0.27	0.23	0.25	0.16
P(N)	1.80	1.81	1.83	1.78
P(Pd)	1.14	1.14	1.14	1.16
N	-1.03	-1.00	-1.43	-1.18
Cl _{trans}	-0.47	-0.46	-0.47	-0.46
Cl _{cis}	-0.54	-0.53	-0.53	-0.51

In modeled complexes **II** as in **I**, the positive charge on Pd was similar for **IIa-c**, while it was lower in **II d** (0.23 a.u). Interestingly, in the latter case this was accompanied by a slight variation of the charge of the Pd-bound carbon and chlorine atoms, which were respectively slightly more positively and less negatively charged. A slight increase of the positive character of the P atom was also observed in **IIc** while this value was subsequently reduced in **II d**. The negative charge on N for **IIc** remained the larger one.

Table 3: Principal NPA charges complexes **IIa-d**. *Cis* and *trans* refer to N.

Complex	IIa	IIb	IIc	II d
Pd	0.33	0.32	0.32	0.23
P(N)	1.81	1.81	1.84	1.79
P(Pd)	1.10	1.11	1.12	1.13
N	-1.05	-1.04	-1.48	-1.23
C _{trans}	0.35	0.36	0.37	0.38
Cl _{cis}	-0.50	-0.50	-0.50	-0.47
N _{trans}	-0.41	-0.41	-0.41	-0.41

The same global observations were made for modeled complexes **IIIa-d**: compound **III d** appeared different. Indeed, the positive charge on Pd was calculated at 0.34 a.u. compared to ~ 0.45 a.u for **IIIa-c**. This effect was also accompanied by the concomitant slight rise of the positive charge accumulation on C_{cis}.

Table 4: Principal NPA charges complexes **IIIa-d**. *Cis* and *trans* refer to N.

Complex	IIIa	IIIb	IIIc	III d
Pd	0.42	0.47	0.46	0.34
P(N)	1.82	1.81	1.83	1.81
P(Pd)	1.11	1.07	1.08	1.11
N	-1.10	-1.07	-1.49	-1.26
C _{trans}	0.30	0.29	0.30	0.33
C _{cis}	0.29	0.28	0.29	0.31
N _{trans}	-0.38	-0.38	-0.38	-0.38
N _{cis}	-0.40	-0.39	-0.40	-0.39

The calculated charges in the series **IIa-d** and **IIIa-d** have showed differences for the H substituted complexes (**II-III d**) compared to the other derivatives. Less markedly, some differences may also be pointed for compounds presenting a TMS substituent. This agrees pretty well with the experimental observations regarding the decreased stability of complexes **2c,d** and **3c,d** compared to the other counterparts.

Conclusion

We synthesized three series of Pd complexes featuring bidentate phosphine-iminophosphorane ligands that differ by the substituent on the N atom (either isopropyl (a), phenyl (b),

trimethylsilyl (c), or H (d)). Starting from the dichloride complexes **1**, the regioselective monosubstitution of one chloride led to complexes **2**, featuring one isocyanide *trans* to the iminophosphorane. The double chloride substitution gave dicationic bis(isocyanide) complexes **3** that exhibited a very low stability in solution particularly in the case of **3c** and **3d** complexes. The differences in complexes **2** concerning the CN frequency and bond length are small but they may suggest a stronger electron backdonation with the isopropyl containing ligand (L^{iPr}). DFT-based molecular modeling was employed to rationalize the experimental observations. First it allowed to explain the seemingly incongruent reactivity of complexes **1**. Indeed, while Pd-Cl_{cis} (*cis* referring to the N atom) was longer in complexes **1**, the substitution led to complexes **2** where the isocyanide was localized in the *trans* position. Molecular modeling showed that, while the *cis* ligand was indeed a better leaving group, the reaction involved a trisubstituted intermediate having lost the original *cis/trans* dissymmetry. From this intermediate, the most stable *trans* isomer formed.

In addition, the analysis of the electronic structure, which was inferred from the calculated atomic charges, showed a rather important effect of the substituent resulting in the modulation of the Pd charge. A difference in the charge of the two chlorine ligands was also observed, again supporting the better leaving group properties of the *cis* atom. The analysis of the electronic distribution suggested stronger similarities between iPr and Ph complexes than TMS and H derivatives.

From our results, alkyl substituted iminophosphoranes appear more suitable to stabilize electron-deficient metal centers while TMS derivative may be more appropriate with electron-rich/less oxidized ones. The subtle influence the iminophosphorane substituent can exert on the electronic properties and the reactivity/stability of PN supported complexes was pointed out; this may help develop their applications.

Experimental Section

General information

atmosphere using a vacuum line, inert Schlenk techniques (N₂) and a glove box (Ar, <0.1 ppm H₂O, <0.1 ppm O₂) with oven-dried glassware unless other notified. L^{iPr}.HBF₄ was as previously reported.^[13] CH₂Cl₂, pentane, diethyl ether and toluene were taken from solvent purification system (MBraun-SPS) and THF was distilled over Na and benzophenone. Deuterated solvents were stored over molecular sieves. All other reagents and chemicals were obtained commercially and used without further purification. NMR spectra were recorded either on a Bruker AC-300 SY spectrometer at 300 MHz for ¹H, 120 MHz for ³¹P and 75 MHz for ¹³C or on a Bruker AC-400 SY spectrometer at 400 MHz for ¹H and 101 MHz for ¹³C or on a Bruker AC-600 SY spectrometer at 600 MHz for ¹H, 243 MHz for ³¹P and 151 MHz for ¹³C. Solvent peaks were used as internal references for ¹H and ¹³C chemical shifts (ppm). ³¹P{¹H} NMR spectra are relative to an 85% H₃PO₄ external reference. Unless otherwise mentioned, NMR spectra were recorded at 300 K. The abbreviations used to indicate the multiplicity of signals are: s (singlet), d (doublet), t (triplet), q (quadruplet), quint (quintuplet), m (multiple) or a combination of the above. The coupling constants *J* were expressed in hertz. The spectra were analyzed with Topspin software. IR spectra were recorded on an IR-TF Thermo Scientific Nicolet iS5 spectrometer. Mass spectrometry experiments were performed on a Tims-TOF mass spectrometer (Bruker, France). Electrospray source has been used in positive and negative modes. Samples are prepared in acetonitrile with 0.1 % formic acid at μM

concentration. 2 to 10 μL were introduced without separation with Elute UHPLC module (Bruker) at a 100 μL min⁻¹ flow rate into the interface of the instrument. Capillary and end plate voltages were set at 4.5 kV and 0.5 kV for ESI experiments. Nitrogen was used as the nebulizer and drying gas at 2 bar and 8 L min⁻¹, respectively, with a drying temperature of 220 °C for ESI source. Tuning mix (Agilent, France) was used for calibration. The elemental compositions of all ions were determined with the instrument software Data Analysis, the precision of mass measurement was less than 3 ppm. Elemental analyses were performed by the elemental analysis service of the Laboratoire de Chimie de Coordination (Toulouse) using a PerkinElmer 2400 series II analyzer. X-ray crystallography data were collected at 150 K on a Bruker Kappa APEX II diffractometer for 1a, 1c, 1d, 2a and 2b or a Stoe Stradivari diffractometer for 1b, 2c and 2d using a Mo-κ (λ = 0.71069Å) X-ray source and a graphite monochromator. The crystal structures were solved using Shelxt33^[22] or olex^[23] and refined using Shelxl-97 or Shelxl-2014.^[24] ORTEP drawings were made using ORTEP III^[25] for Windows. Details of crystal data and structure refinements are summarized in Table S1-3.

Computational Modeling

Molecular modeling was performed at the density functional theory (DFT) level using consistently the ORCA 4.2.1 code.^[26] Geometry optimization was performed with the help of the B3LYP exchange–correlation functional^[27] adding Grimme dispersion corrections^[28] and the Def2-SVP basis set^[29], including pseudopotential for heavy atoms (palladium). The vibrational frequencies have been obtained within the harmonic approximation by diagonalizing the hessian matrix, calculated at the same level of theory as for the geometry optimization. Dichloromethane solvent was implicitly taken into account in all calculations using the conductor-like Polarizable Continuum Model (CPCM) as implemented in ORCA 4.^[30] The same level of theory, i.e., B3LYP/Def2-SVP, has been used to compute the relaxed scan along the Pd-Cl elongation from the equilibrium distance to 5.5 Å via consecutive steps of 0.2 Angstroms. The Natural population analysis (NPA) charges for all the complexes have been calculated at the DFT level using TERACHEM V1.93P^[31] and the NBO 6.0 code^[32] using B3LYP exchange–correlation functional including dispersion correction and the LANL2DZ^[33] double zeta basis set.

Syntheses

L^{TMS}: BuLi (1.61 mL, 2.42 mmol) was added to a solution of PPh₃NTMS (0.778 g, 2.2 mmol) in Et₂O (15 mL) at -78°C. The cold bath was removed and stirring was pursued 30 min leading to a light-yellow solution exhibiting a singlet at 19 ppm by ³¹P{¹H} spectroscopy. The reaction mixture was cooled back to -78°C and PPh₂Cl (0.4 mL, 2.2 mmol), 2.2 mmol) was added leading to a white suspension. Stirring was pursued 1h30, and the solvent was evaporated. The product was extracted with CH₂Cl₂ (20 mL). Then, this solvent was removed and the solid was washed with Et₂O (2x10 mL) to give **L^{TMS}** (728 mg, 1.36 mmol, 62 %). ³¹P NMR (CD₂Cl₂, 121.5 MHz): δ = -15.5 (d, J_{P,P} = 17.5 Hz, P^{III}) and 1.2 (d, J_{P,P} = 17.5 Hz, PN); ¹H NMR (CD₂Cl₂, 300 MHz): δ = 7.65 (dd, J_{H,H} = 8.0 and 1.5 Hz and J_{P,H} = 12.5 Hz, 4H, CH_{PPH2}), 7.52-7.35 (m, 9H, CH_{ArP2} and CH_{PPH2}), 7.33-7.20 (m, 7H, CH_{ArP2} and CH_{PPH2}), 7.01 ddd, J_{H,H} = 8.0 and 1.5 Hz and J_{P,H} = 7.0 Hz, 4H, CH_{PPH2}), -0.15 (s, 9H). Data were in agreement with the literature.^[14b]

L^{Ph}: Phenyl azide (260.8 mg, 2.2 mmol) was added to a white suspension of 1,2 bis diphenylphosphinobenzene (937.7 mg, 2.1 mmol) in toluene (10 mL). The suspension immediately turned brown and was heated to reflux, turning into a clear brown solution after one day. After 4 days the solution was cooled to room temperature and a heavy precipitate appeared. The precipitate was filtered then dried under vacuum to give a beige powder (715.8 mg, 1.3 mmol, 63%). ³¹P NMR (CD₂Cl₂, 243 MHz): δ = -15.1 (d, J_{P,P} = 22.0 Hz, P^{III}) and 3.6 (d, J_{P,P} = 22.0 Hz, PN); ¹H NMR (CD₂Cl₂, 700 MHz): δ = 7.74 (dd, J_{H,H} = 8.0 and J_{P,H} = 12.0 Hz, 4H, CH_{PPH2}), 7.58 (m, 1H, CH_{ArP2}), 7.45 (m, 4H, CH_{PPH2} and CH_{NPh}), 7.35 (td, J_{H,H} = 7.5 Hz and J_{P,H} = 2.5 Hz, 4H, CH_{PPH2}), 7.32 (dd, J_{H,H} = 7.0 Hz and J_{P,H} = 3.5 Hz, 1H, CH_{ArP2}), 7.22 (t, J_{H,H} = 7.5 Hz, 2H, CH_{PPH2}), 7.15 (t, J_{H,H} = 7.5 Hz, 4H, CH_{PPH2}), 6.88 (t, J_{H,H} = 7.5 Hz, 2H, CH_{NPh}), 6.84 (vt, J_{H,H} = J_{P,H} = 7.5 Hz, 4H, CH_{PPH2}), 6.55 (t, J_{H,H} = 7.0 Hz, 1H, CH_{ArP2}), 6.48 (d, J_{H,H} = 8.0 Hz, 1H, CH_{NPh}); ¹³C{¹H} NMR (CD₂Cl₂, 175 MHz): δ = 152.1 (s, C_{NPh}), 143.1 (dd, J_{P,C} = 20.0 and 9.0

Hz, C_{ArP2}), 138.6 (d, J_{P,C} = 8.5 Hz, CH_{ArP2}), 138.3 (dd, J_{P,C} = 56.0 and 27.0 Hz, C_{ArP2}), 138.2 (d, J_{P,C} = 13.0 Hz, C_{PPH2}), 135.0 (dd, J_{P,C} = 11.0 and 8.0 Hz, CH_{ArP2}), 133.5 (d, J_{P,C} = 17.0 Hz, CH_{PPH2}), 133.0 (d, J_{P,C} = 8.0 Hz, CH_{PPH2}), 132.9 (d, J_{P,C} = 86.0 Hz, C_{PPH2}), 132.0 (d, J_{P,C} = 1.0 Hz, CH_{PPH2}), 131.8 (d, J_{P,C} = 1.0 Hz, CH_{ArP2}), 129.4 (d, J_{P,C} = 10.0 Hz, CH_{ArP2}), 129.0 (d, J_{P,C} = 5.0 Hz, CH_{NPh}), 128.9 (s, CH_{PPH2}), 128.6 (d, J_{P,C} = 1.5 Hz, CH_{PPH2}), 128.5 (s, CH_{PPH2}), 123.6 (d, J_{P,C} = 16.0 Hz, CH_{NPh}), 117.3 (s, CH_{NPh}). HRMS (ESI⁺): calculated for [C₃₆H₃₀NP₂]⁺ ([L^{Ph}H]⁺): 538.1848; found: 538.1848. Elemental analysis for C₃₆H₂₉NP₂: calc (%) C 80.43; H 5.44; N 2.61; found C 80.41; H 5.18; N 2.60.

[Pd(L^{Ph})Cl₂] **1a**: KHMDS (200 mg, 1 mmol) was added to a solution of L^{Ph}, HBF₄ (591.4 mg, 1 mmol) in THF (40 mL), the suspension rapidly turned into a clear yellow solution. The ³¹P NMR analysis of the crude mixture shows the formation of L (δ_P = -1.18 and -13.67, J_{P,P} = 13.0 Hz). The slight suspension was filtered through a PTFE filter, THF was removed under vacuum and the obtained yellow solid was dissolved in CH₂Cl₂ (30 mL) and added through a canula to [Pd(COD)Cl₂] (285.5 mg, 1 mmol), the reaction mixture was stirred 2 h at room temperature, inducing the formation of an orange precipitate. The mixture was concentrated by evaporation of half the solvent and the supernatant was removed by cannulation. The obtained yellow solid was washed with THF (2x5 mL) and dried under vacuum to give a **1a** as a bright yellow solid (595 mg, 87%). IR (neat, cm⁻¹): 1436, 1175, 1112, 1090. ³¹P{¹H} NMR (CD₂Cl₂, 121.5 MHz): δ = 11.9 (d, J_{P,P} = 35.5 Hz, PN), 22.4 (d, J_{P,P} = 35.5 Hz, P^{III}); ¹H NMR (CD₂Cl₂, 300 MHz): δ = 7.61-7.82 (m, 6H, CH_{PPH2}), 7.33-7.59 (m, 14 H, CH_{PPH2} and CH_{ArP2}), 7.19-7.29 (m, 4H, CH_{PPH2}), 3.17 (hept, J_{H,H} = 7.0 Hz, 1H, CH(CH₃)₂), 1.02 (d, J_{H,H} = 6.5 Hz, 6H, CH(CH₃)₂); ¹³C{¹H} NMR (CD₂Cl₂, 75 MHz): δ = 137.4 (d, J_{P,C} = 8.5 Hz, CH_{ArP2}), 135.0 (dd, J_{P,C} = 9.0 and 10.0 Hz, CH_{ArP2}), 134.6 (d, J_{P,C} = 10.5 Hz, CH_{PPH2}), 133.8 (d, J_{P,C} = 11.0 Hz, CH_{PPH2}), 134.2 (s, C_{Ar}), 133.6 (d, J_{P,C} = 2.5 Hz, CH_{PPH2}), 132.8 (dd, J_{P,C} = 6.5 et 2.5 Hz, CH_{ArP2}), 132.3 (d, J_{P,C} = 7.5 Hz, C_{ArP2}), 130.9 (d, J_{P,C} = 2.5 Hz, CH_{PPH2}), 130.4 (d, J_{P,C} = 11.0 Hz, CH_{ArP2}), 129.2 (d, J_{P,C} = 12.5 Hz, CH_{PPH2}), 128.4 (d, J_{P,C} = 11.5 Hz, CH_{PPH2}), 127.0 (d, J_{P,C} = 104.5 Hz, C_{PPH2}), 50.2 (s, CH_{IPr}), 26.9 (d, J_{P,C} = 7.0 Hz, CH_{3IPr}). HRMS (ESI⁺): calculated for [C₃₃H₃₁CINP₂Pd]⁺ ([**1a**-Cl]⁺): 644.0650; found: 644.0661. Elemental analysis for C₃₃H₃₁ClNP₂Pd: calc (%) C 58.21; H 4.59; N 2.06; found C 58.23; H 4.18; N 2.14.

[Pd(L^{Ph})Cl₂] **1b**: L^{Ph} (164.1 mg, 0.3 mmol) was dissolved in THF (10 mL) and added to PdCl₂·COD (85.7 mg, 0.3 mmol). Upon stirring the solution turned turbid after 15 minutes. The stirring was stopped after 2 days and the orange precipitate was filtered then washed with Et₂O (2 x 5 mL) before being dried under vacuum to give [Pd(L^{Ph})Cl₂] as a yellow solid (207.2 mg, 0.28 mmol, 94%). IR (neat, cm⁻¹): 1481, 1433, 1251, 1108, 1096, 1034, 994. ³¹P NMR (CD₂Cl₂, 243 MHz): δ = 11.9 (d, J_{P,P} = 26.5 Hz, PN) and 23.5 (d, J_{P,P} = 26.5 Hz, P^{III}); ¹H NMR (600 MHz, CD₂Cl₂): δ = 7.71 (vtq, J_{H,H} = 7.5 Hz, J_{H,H} = J_{P,H} = 1.0 Hz, 1H, CH_{ArP2}), 7.62 (td, J_{H,H} = 7.5 Hz and J_{P,H} = 1.5 Hz, 2H, CH_{PPH2}), 7.57-7.59 (m, 6H, CH_{PPH2}), 7.54 (dt, J_{H,H} = 8.0 Hz and J_{P,H} = 1.5 Hz, 1H, CH_{ArP2}), 7.43-7.50 (m, 5H, CH_{PPH2} and CH_{ArP2}), 7.45 (m, 4H, CH_{PPH2}), 7.40 (td, J_{H,H} = 7.5 Hz and J_{P,H} = 3.5 Hz, 4H, CH_{PPH2}), 7.30 (oct, J_{H,H} = 7.5 and J_{P,H} = 5.0 Hz, 1H, CH_{ArP2}), 6.95-6.97 (m, 3H, CH_{NPh}), 6.87 (dt, J_{H,H} = 2.5 and J_{H,H} = 7.5 Hz, 2H, CH_{NPh}). ¹³C{¹H} NMR (150 MHz, CD₂Cl₂): δ = 145.2 (d, J_{P,C} = 2.5 Hz, C_{NPh}), 137.5 (d, J_{P,C} = 8.5 Hz, CH_{ArP2}), 135.8 (s, CH_{ArP2}), 134.9 (d, J_{P,C} = 12.0 Hz, CH_{PPH2}), 134.8 (d, J_{P,C} = 12.0 Hz, CH_{PPH2}), 134.3 (d, J_{P,C} = 2.0 Hz, CH_{PPH2}), 133.8 (s, CH_{ArP2}), 131.7 (d, J_{P,C} = 2.5 Hz, CH_{ArP2}), 131.6 (d, J_{P,C} = 5.5 Hz, CH_{PPH2}), 131.3 (s, CH_{NPh}), 131.2 (s, C_{ArP2}), 130.4 (s, C_{ArP2}), 129.6 (d, J_{P,C} = 13.0 Hz, CH_{NPh}), 129.1 (d, J_{P,C} = 12.5 Hz, CH_{PPH2}), 129.0 (d, J_{P,C} = 58.5 Hz, C_{PPH2}), 128.8 (d, J_{P,C} = 1.5 Hz, CH_{NPh}), 125.2 (d, J_{P,C} = 108.0 Hz, C_{PPH2}), 124.8 (s, CH_{NPh}). HRMS (ESI⁺): calculated for [C₃₆H₂₉NP₂PdCl]⁺ ([**1b**-Cl]⁺): 678.0493; found: 678.0500. Elemental analysis for C₃₆H₂₉ClNP₂Pd (0.4 CH₂Cl₂): calc (%) C 60.48; H 4.01; N 1.87; found C 58.34; H 4.01; N 2.11.

[Pd(L^{TMS})Cl₂] **1c**: L^{TMS} (533.7 mg, 1 mmol) was dissolved in THF (25 mL) and added to [PdCl₂(COD)] (285.5 mg, 1 mmol). After few minutes stirring the solution turned turbid after. After 24 h, the stirring was stopped and the orange precipitate was filtered and washed with Et₂O (2 x 12 mL) before being dried under vacuum to give [Pd(L^{TMS})Cl₂] as a yellow solid (576.8 mg, 0.8 mmol, 80%). IR (neat, cm⁻¹): 1436, 1247, 1119, 1088. ³¹P NMR (CD₂Cl₂, 121.5 MHz): δ = 15.8 (d, J_{P,P} = 14.5 Hz, PN) and 20.5 (d, J_{P,P} = 14.5 Hz, P^{III}); ¹H NMR (300 MHz, CD₂Cl₂): δ = 8.24 (m, 2H, CH_{PPH2}), 7.89 (m, 2H, CH_{PPH2}), 7.79 (m, 1H, CH_{ArP2}), 7.55-7.75 (m, 8H, CH_{PPH2}), 7.44-7.50 (m, 5H, CH_{ArP2} and CH_{PPH2}), 7.38 (m, 1H, CH_{ArP2}), 7.13-7.33 (m, 5H, CH_{PPH2} and CH_{ArP2}), -0.14 (s, 9H, CH_{TMS}); ¹³C{¹H} NMR (CD₂Cl₂, 125 MHz): δ = 138.5 (d, J_{P,C} = 10.5 Hz, CH_{PPH2}), 135.6 (dd, J_{P,C} = 12.5 and 9.0 Hz, C_{ArP2}), 135.0 (d, J_{P,C} = 13.5 Hz, CH_{PPH2}), 134.8 (d, J_{P,C} = 11.5 Hz, CH_{PPH2}), 133.8 (d, J_{P,C} = 3.0 Hz, CH_{PPH2}), 133.2 (dd, J_{P,C} = 7.0 and 3.0 Hz, CH_{ArP2}), 132.5 (d, J_{P,C} = 7.0 Hz, C_{ArP2}), 132.2 (d, J_{P,C} = 7.0 Hz, CH_{PPH2}), 130.8 (dd, J_{P,C} = 12.5 and 2.5 Hz, CH_{ArP2}), 129.7 (d, J_{P,C} = 12.5 Hz, CH_{PPH2}), 128.8 (d, J_{P,C} = 12.0 Hz, CH_{ArP2}), 128.3 (s, CH_{ArP2}), 127.8 (d, J_{P,C} = 56.5 Hz, C_{PPH2}), 125.6 (d, J_{P,C} = 114.5 Hz, C_{PPH2}), 5.4 (s, CH_{TMS}). HRMS (ESI⁺):

calculated for [C₃₃H₃₃NP₂PdCl]⁺ [**1c**-Cl]⁺: 674.0585; found: 674.0575. Elemental analysis for C₃₃H₃₃ClNP₂PdSi: calc (%) C 55.75; H 4.68; N 1.97; found C 55.74; H 4.27; N 1.92.

[Pd(L^H)Cl₂] **1d**: Methanol (6 mL) was added to a solution of **2c** (144.4 mg, 0.2 mmol) in CH₂Cl₂ (4 mL). After 15 minutes stirring the yellow solution turned turbid and some gray particles appeared. The reaction was stopped after 2 days when the ³¹P NMR monitoring no longer showed the ³¹P resonances corresponding to the starting material. The yellow suspension was filtered and the light-yellow solid covered in gray particles was isolated. Extraction with CHCl₃ (10 mL) and filtration on celite, followed by vacuum evaporation of the solvents give a light-yellow powder (97.6mg, 0.15 mmol, 77%). IR (neat, cm⁻¹): 1435, 1114, 1099, 1005, 994. ³¹P NMR (CDCl₃, 121.5 MHz): δ = 17.7 (d, J_{P,P} = 28.5 Hz, PN) and 32.6 (d, J_{P,P} = 28.5 Hz, P); ¹H NMR (CDCl₃, 600 MHz): δ = 7.64 (dt, 1H, J_{P,H} = 1.0 and J_{H,H} = 75 Hz, 1H, CH_{ArP2}), 7.54 (m, 5H, CH_{ArP2} and CH_{PPH2}), 7.52 (d, J_{H,H} = 8.0 Hz, 4H, CH_{PPH2}), 7.50 (d, J_{H,H} = 7.5 Hz, 2H, CH_{PPH2}), 7.32-7.39 (m, 6H, CH_{PPH2}), 7.31 (m, 1H, CH_{ArP2}), 7.22 (dt, J_{P,H} = 2.5 and J_{H,H} = 8.0 Hz, 1H, CH_{PPH2}), 7.18 (m, 1H, CH_{ArP2}), the NH resonance was not seen; ¹³C{¹H} NMR (CDCl₃, 150 MHz): δ = 136.4 (d, J_{P,C} = 9.0 Hz, CH_{ArP2}), 134.6 (d, J_{P,C} = 12.0 Hz, CH_{PPH2}), 134.0 (dd, J_{P,C} = 9.0 and 12.5 Hz, CH_{ArP2}), 133.8 (d, J_{P,C} = 3.0 Hz, CH_{PPH2}), 133.2 (s, CH_{PPH2}), 133.1 (d, J_{P,C} = 11.0 Hz, CH_{ArP2}), 132.6 (dd, J_{P,C} = 3.0 and 109.5 Hz, C_{ArP2}), 132.4 (dd, J_{P,C} = 5.5 and 38.0 Hz, C_{ArP2}), 131.2 (d, J_{P,C} = 3.0 Hz, CH_{PPH2}), 130.8 (dd, J_{P,C} = 2.5, 13.5 Hz, CH_{ArP2}), 129.4 (d, J_{P,C} = 12.5 Hz, CH_{PPH2}), 128.5 (d, J_{P,C} = 12.0 Hz, CH_{PPH2}), 128.2 (d, J_{P,C} = 87.0 Hz, C_{PPH2}), 128.0 (d, J_{P,C} = 66.5 Hz, C_{PPH2}). HRMS (ESI⁺): calculated for [C₃₀H₂₅CINP₂Pd]⁺ [**1d**-Cl]⁺: 602.0180; found: 602.0187. Elemental analysis for C₃₀H₂₅ClNP₂Pd (0.2 CH₂Cl₂): calc (%) C 55.31; H 3.90; N 2.14; found C 55.37; H 2.88; N 2.15.

[Pd(L^{IPr})(CN^tBu)Cl](OTf) **2a**: A solution of AgOTf (25.7 mg, 0.1 mmol) in a mixture of CH₂Cl₂:CH₃CN (10:1, 4.5 mL) was added to [L^{IPr}PdCl₂] (0.1 mmol, 68.1 mg). After stirring 20 min at room temperature, the precipitate was filtered off thanks to a PTFE filter and a solution of tertbutyl isocyanide (0.1 mmol, 667 μL of a 0.15 M solution in CH₂Cl₂:CH₃CN (10:1), 0.1 mmol) was added to the filtrate. After stirring 30 min at room temperature, the solvent was removed and the product was isolated after washing with Et₂O (2x3 mL) [Pd(L^{IPr})(CN^tBu)Cl] as a yellow solid (53 mg, 60%). IR (neat, cm⁻¹): 2227, 1436, 1262, 1222, 1142, 1110, 1029, 997. RMN ³¹P{¹H} (CD₂Cl₂, 121.5 MHz): δ = 14.1 (d, J_{P,P} = 34.5 Hz, PN), 26.0 (d, J_{P,P} = 34.5 Hz, P); RMN ¹H (CD₂Cl₂, 300 MHz): δ = 7.75-7.80 (m, 4H, CH_{PPH2}), 7.58-7.74 (m, 10H, CH_{PPH2} and CH_{ArP2}), 7.49-7.57 (m, 5H, CH_{PPH2} and CH_{ArP2}), 7.32-7.41 (m, 5H, CH_{PPH2} and CH_{ArP2}), 3.28 (sept, J_{H,H} = 7.0 Hz, 1H, CH_{IPr}), 1.09 (s, 9H, CH_{3CNBu}), 0.98 (d, J_{H,H} = 6.5 Hz, 6H, CH_{3IPr}). RMN ¹³C{¹H} (CD₂Cl₂, 75 MHz): δ = 140.8 (s, CN₃Bu), 137.6 (dd, J_{P,C} = 2.5 and 8.5 Hz, CH_{ArP2}), 135.9 (dd, J_{P,C} = 9.5 and 11.0 Hz, CH_{ArP2}), 135.5 (d, J_{P,C} = 16.0 Hz, C_{ArP2}), 134.9 (d, J_{P,C} = 10.5 Hz, CH_{PPH2}), 134.6 (d, J_{P,C} = 3.0 Hz, CH_{ArP2}), 134.3 (dd, J_{P,C} = 2.5 and 8.5 Hz, CH_{PPH2}), 133.4 (d, J_{P,C} = 11.5 Hz, CH_{PPH2}), 133.2 (d, J_{P,C} = 3.0 Hz, CH_{ArP2}), 132.7 (dd, J_{P,C} = 2.5 and 11.5 Hz, CH_{PPH2}), 130.2 (d, J_{P,C} = 12.0 Hz, CH_{PPH2}), 129.9 (d, J_{P,C} = 12.5 Hz, CH_{PPH2}), 129.0 (d, J_{P,C} = 58.0 Hz, C_{PPH2}), 126.0 (d, J_{P,C} = 105.0 Hz, C_{PPH2}), 125.9 (s, C_{ArP2}), 60.2 (s, CN₃Bu), 51.6 (s, CH_{IPr}), 29.3 (s, CH_{IPr}), 27.2 (s, CH_{3CNBu}). HRMS (ESI⁺): calculated for [C₃₈H₄₀CIN₂P₂Pd]⁺ ([Pd(L^{IPr})(CN^tBu)Cl]⁺): 727.1393; found: 727.1385. Elemental analysis for C₃₈H₄₀ClF₃N₂O₃P₂PdSi (0.2 CH₂Cl₂): calc (%) C 52.63; H 4.55; N 3.13; found C 52.77; H 4.18; N 3.24.

[Pd(L^{Ph})(CN^tBu)Cl](OTf) **2b**: A solution of [L^{Ph}PdCl₂] (59.0 mg, 0.08 mmol) in CH₂Cl₂ (3 mL) was added to AgOTf (20.6 mg, 0.08 mmol). Upon stirring the yellow solution turned turbid after 5 minutes and a gray precipitate appeared. The stirring was stopped after 2 h, the precipitate was filtered off thanks to a PTFE filter. A solution of tertbutyl isocyanide (0.08 mmol, 170 μL, 0.47 M solution in CH₂Cl₂, 0.047 mmol) was added to the orange filtrate which immediately turned light-yellow. After 2 hours of stirring, the solvent was evaporated under vacuum giving a light yellow oil which was washed with Et₂O (2 x 5 mL) before being dried under vacuum to give [Pd(L^{Ph})(CN^tBu)Cl] as a light-yellow powder (53.5 mg, 0.058 mmol, 73%). IR (neat, cm⁻¹): 2234, 1481, 1436, 1265, 1142, 1118, 1108, 1030, 993. ³¹P NMR (300 MHz, CD₂Cl₂): δ = 14.5 (d, J_{P,P} = 39.5 Hz) and 26.4 (d, J_{P,P} = 39.5 Hz); ¹H NMR (CD₂Cl₂, 600 MHz): δ = 7.90 (td, J_{H,H} = 7.5 Hz and J_{H,H} = 1.0 Hz, 1H, CH_{ArP2}), 7.79 (t, J_{H,H} = 8.0 Hz, 1H, CH_{ArP2}), 7.65 (m, 4H, CH_{PPH2}), 7.53 (td, J_{H,H} = 7.5 Hz and J_{P,H} = 3.0 Hz, 4H, CH_{PPH2}), 7.47 (m, 2H, CH_{ArP2}), 7.42-7.44 (m, 4H, CH_{PPH2}), 7.41 (m, 4H, CH_{PPH2}), 7.36-7.38 (m, 4H, CH_{PPH2}), 6.99 (m, 3H, CH_{NPh}), 6.71 (vtd, J_{H,H} = 7.5 and J_{P,H} = 1.5 Hz, 2H, CH_{NPh}), 1.05 (s, 9H, CH_{3CNBu}); ¹³C{¹H} NMR (CD₂Cl₂, 150 MHz): δ = 144.4 (s, CN₃Bu), 137.5 (d, J_{P,C} = 7.5 Hz, CH_{ArP2}), 136.7 (d, J_{P,C} = 8.5 Hz, CH_{ArP2}), 135.1 (s, CH_{PPH2}), 135.0 (d, J_{P,C} = 2.5 Hz, CH_{ArP2}), 134.8 (d, J_{P,C} = 7.0 Hz, CH_{PPH2}), 134.6 (d, J_{P,C} = 13.0 Hz, C_{ArP2}), 134.1 (d, J_{P,C} = 12.0 Hz, CH_{PPH2}), 133.6 (d, J_{P,C} = 2.0 Hz, CH_{PPH2}), 133.3 (d, J_{P,C} = 10.5 Hz, CH_{ArP2}), 130.9 (d, J_{P,C} = 6.0 Hz, CH_{NPh}), 130.6 (d, J_{P,C} = 12.0 Hz, CH_{PPH2}), 129.9 (d, J_{P,C} = 13.5 Hz, CH_{PPH2}), 129.6 (dd, J_{P,C} = 12.0 Hz, C_{ArP2}), 129.4 (d, J_{P,C} = 3.0 Hz, C_{NPh}), 129.1 (s, CH_{NPh}), 128.1 (d, J_{P,C} = 56.0 Hz, C_{PPH2}), 125.7 (s,

CH₃NH), 124.4 (d, J_{P,C}= 103.0 Hz, C_{PPH2}), 55.3 (s, C_{IBu}), 29.5 (s, CH₃IBu). calculated for [C₄₁H₃₈ClN₂P₂Pd]⁺ ([Pd(L^{Ph})(CN^{Bu})Cl]⁺): 761.1210; found: 761.1228. Elemental analysis for C₄₅H₃₈ClF₃N₂O₃P₂PdS₂ (0.3 CH₂Cl₂): calc (%) C 54.22; H 4.15; N 2.99; found C 53.93; H 3.89; N 2.96.

[Pd(L^{TMS})(CN^{Bu})Cl](OTf) **2c**: A solution of [Pd(L^{TMS})Cl₂] (33.7 mg, 0.047 mmol) in dichloromethane (2 mL) was added to AgOTf (12.1 mg, 0.047 mmol). Upon stirring the yellow solution turned turbid after 5 minutes and a gray precipitate appeared. The stirring was stopped after 1h30 the precipitate was filtered off thanks to a PTFE filter. A solution of tertbutyl isocyanide (100 μL, 0.47 M solution of ^tBuNC in CH₂Cl₂, 0.047 mmol) was added to the orange filtrate which immediately turned light-yellow. After 10 min. stirring, the solvent was evaporated under vacuum and the yellow oil was washed with Et₂O (4 mL) before being dried under vacuum to give a light-yellow powder (28.3 mg, 0.031 mmol, 66%). IR (neat, cm⁻¹): 2229, 1436, 1264, 1111, 1030. ³¹P NMR (CD₂Cl₂, 243 MHz): δ = 19.4 (d, J_{P,P}= 20.5 Hz) and 26.6 (d, J_{P,P}= 20.5 Hz); ¹H NMR (CD₂Cl₂, 600 MHz): δ = 8.15 (m, 1H, CH_A), 8.00 (m, 1H, CH_{Ar}), 7.82 (m, 4H, CH_{PPH2}), 7.74 (m, 4H, CH_{NPPH2}), 7.58-7.62 (m, 4H, CH_{PPH2}), 7.55 (m, 2H, CH_{Ar}), 7.38-7.42 (m, 2H, CH_{PPH2}), 7.36 (vtd, J_{H,H}= 7.0 Hz, J_{P,H}= 1.0 Hz, 4H, CH_{PPH2}), 7.27 (m, 2H, CH_{PPH2}), 1.10 (s, 9H, CH_{CNIBu}), -0.22 (s, 9H, CH_{TMS}). ¹³C{¹H} NMR (CD₂Cl₂, 150 MHz): δ = 145.6 (s, C_{CNIBu}), 138.2 (dd, J_{P,C}= 3.5 Hz and 10.0 Hz, CH_{PPH2}), 136.7 (dd, J_{P,C}= 9.5 Hz and 12.5 Hz, CH_{ArP2}), 136.6 (dd, J_{P,C}= 4.0 Hz and 10.5 Hz, C_{ArP2}), 135.3 (s, CH_{ArP2}), 134.9 (d, J_{P,C}= 7.5 Hz, CH_{PPH2}), 133.7 (d, J_{P,C}= 2.5 Hz, CH_{PPH2}), 133.1 (s, CH_{PPH2}), 132.9 (d, J_{P,C}= 12.0 Hz, CH_{PPH2}), 132.6 (d, J_{P,C}= 12.0 Hz, C_{ArP2}), 131.5 (s, CH_{ArP2}), 130.4 (d, J_{P,C}= 13.5 Hz, CH_{PPH2}), 129.7 (d, J_{P,C}= 10.5 Hz, CH_{ArP2}), 127.3 (d, J_{P,C}= 54.0 Hz, C_{PPH2}), 126.9 (d, J_{P,C}= 96.5 Hz, C_{PPH2}) 54.9 (s, C_{IBu}), 29.7 (s, J_{P,C}= 7.5 Hz, CH₃IBu), 5.8 (d, J_{P,C}= 2.5 Hz, CH_{TMS}). HRMS (ESI⁺): calculated for [C₃₈H₄₂ClN₂P₂PdSi]⁺ [Pd(L^{TMS})(CN^{Bu})Cl]⁺: 761.1210; found: 761.1228; calculated for [C₃₉H₄₂F₃N₂O₃P₂PdSSi]⁺ ([Pd(L^{TMS})(CN^{Bu})(OTf)]⁺): 871.1142; found: 871.1118. Elemental analysis for C₃₉H₄₂ClF₃N₂O₃P₂PdSSi: calc (%) C 51.60; H 4.66; N 3.09; found C 51.62; H 5.21; N 3.39.

[Pd(L^H)(CN^{Bu})Cl](OTf) **2d**: A solution of [Pd(L^H)Cl₂] (31.6 mg, 0.047 mmol) in dichloromethane (2 mL) was added to TIOtF (16.6 mg, 0.047 mmol). Upon stirring the yellow solution turned turbid after 5 minutes and a gray precipitate appeared. The stirring was stopped after 1h30 the precipitate was filtered off thanks to a PTFE filter. A solution of tertbutyl isocyanide (100 μL, 0.47 M solution of ^tBuNC in CH₂Cl₂, 0.047 mmol) was added to the orange filtrate which immediately turned light-yellow. After 5 min. stirring, the solvent was evaporated under vacuum giving a yellow oil which was washed with Et₂O (4 mL) before being dried under vacuum to give [Pd(L^H)(CN^{Bu})Cl] as a light-yellow powder (26.5 mg, 0.033 mmol, 68%). IR (neat, cm⁻¹): 2228, 1437, 1262, 1144, 1111, 1029. ³¹P NMR (CD₂Cl₂, 121.5 MHz): δ = 22.2 (d, J_{P,P}= 33.5 Hz) and 33.0 (d, J_{P,P}= 33.5 Hz); ¹H NMR (300 MHz, CD₂Cl₂): δ = 7.81 (m, 2H, CH_{ArP2}), 7.62 (m, 4H, CH_{PPH2}), 7.41 (m, 18H, CH_{ArP2} and CH_{PPH2}), 1.16 (s, 9H, CH_{CNIBu}), the NH resonance was not seen. ¹³C-NMR (CD₂Cl₂, 101 MHz): δ = 142.7 (s, C_{CNIBu}), 136.4 (dd, J_{P,C}= 3.5 and 8.5 Hz, CH_{ArP2}), 135.6 (t, J_{P,C}=10.5 Hz, CH_{PPH2}), 134.7 (d, J_{P,C}= 3.0 Hz, CH_{PPH2}), 134.4 (dd, J_{P,C}=2.5 and 8.0 Hz, CH_{ArP2}), 134.2 (d, J_{P,C}=12.5 Hz, CH_{PPH2}), 133.7 (d, J_{P,C}= 9.0 Hz, CH_{PPH2}), 133.5 (d, J_{P,C}= 3.0 Hz, CH_{PPH2}), 133.2 (d, J_{P,C}= 1.0 Hz, CH_{PPH2}), 133.0 (dd, J_{P,C}= 3.0 and 12.0 Hz, CH_{ArP2}), 130.1 (dd, J_{P,C}=12.5 and 19.5 Hz, CH_{ArP2}), 129.2 (s, C_{ArP2}), 128.8 (d, J_{P,C}= 58.0 Hz, C_{PPH2}), 126.6 (d, J_{P,C}=18.0 Hz, C_{ArP2}), 126.9 (d, J_{P,C}= 99.5 Hz, C_{PPH2}), 52.9 (s, C_{CNIBu}), 29.5 (s, CH_{CNIBu}). HRMS (ESI⁺): calculated for [C₃₅H₃₄ClN₂P₂Pd]⁺ ([Pd(L^H)(CN^{Bu})Cl]⁺): 685.0921; found: 685.0915. Elemental analysis for C₃₆H₃₄ClF₃N₂O₃P₂PdS₂ (0.2 CH₂Cl₂): calc (%) C 51.00; H 4.07; N 3.29; found C 50.91; H 4.01; N 3.85.

[Pd(L^{Ph})(CN^{Bu})₂](OTf)₂ **3a**: A solution of AgOTf (0.2 mmol ; 51.4 mg) in a mixture of CH₂Cl₂:CH₃CN (10:1, 4 mL) was added to **1a** (0.1, 68.1 mg). After stirring 20 min at room temperature, the precipitate is filtered off thanks to a PTFE filter and tertbutyl isocyanide (0.6 mmol, 68 μL) was added to the reaction mixture. After stirring 30 min at room temperature the solvent is removed and the product is isolated as a yellow green solid (79.4 mg, 74%). IR (neat, cm⁻¹): 2981, 2239, 2199, 1586, 1438, 1262, 1189, 1145, 1113, 1028, 998. RMN ¹³P{¹H} (CD₂Cl₂, 121.5 MHz): δ = 10.5 (d, J_{P,P} = 32.5 Hz Hz, PN), 29.9 (d, J_{P,P} = 32.5 Hz, P); RMN ¹H (CD₂Cl₂, 300 MHz) : δ = 7.80-7.88 (m, 4H, CH_{PPH2}), 7.76-7.76 (m, 1H, CH_{ArP2}), 7.41-7.76 (m, 18H, CH_{PPH2} and CH_{ArP2}), 7.34-7.38 (m, 1H, CH_{ArP2}), 3.29 (sept, J_{H,H}= 7.0 Hz, 1H, CH_{IPr}), 1.66 (s, 9H, CH_{CNIBu}), 1.17 (s, 9H, CH_{CNIBu}), 0.95 (d, J_{H,H}= 6.5 Hz, 6H, CH₃IPr) ; RMN ¹³C{¹H} (CD₂Cl₂, 75 MHz) : δ = 144.1 (s, C_{CNIBu}), 141.0 (s, C_{CNIBu}), 139.0 (d, J_{P,C}= 12.0 Hz, CH_{ArP2}), 137.0 (d, J_{P,C}= 12.0 Hz, C_{ArP2}), 135.0 (d, J_{P,C}= 3.0 Hz, CH_{ArP2}), 134.7 (s, CH_{PPH2}), 133.6 (s, CH_{ArP2}), 133.5 (s, CH_{PPH2}), 133.4 (s, CH_{PPH2}), 133.3 (d, J_{P,C}= 3.0 Hz, CH_{PPH2}), 133.0 (d, J_{P,C}= 17.5 Hz, CH_{PPH2}), 130.8 (s, C_{ArP2}), 130.3 (d, J_{P,C}= 8.5 Hz, CH_{ArP2}), 130.1 (d, J_{P,C}= 9.5 Hz, CH_{PPH2}), 126.6 (d, J_{P,C}= 58.0 Hz, C_{PPH2}), 124.5 (d, J_{P,C}= 104.5 Hz, C_{PPH2}), 57.2 (s, C_{CNIBu}), 54.5 (s, C_{CNIBu}), 47.4 (s, CH_{IPr}), 28.3 (s, CH_{CNIBu}), 27.4 (s, CH_{CNIBu}), 25.2 (d, J_{P,C}= 6.5 Hz, CH₃IPr). HRMS (ESI⁺): calculated for [C₃₉H₄₀F₃N₂O₃P₂PdS]⁺ ([Pd(L^{Ph})(CN^{Bu})(OTf)]⁺):

841.1216; found: 841.1206; calculated for [C₄₄H₅₁F₃N₃O₃P₂PdS]⁺ ([Pd(L^{Ph})(CN^{Bu})₂H₂(OTf)]⁺): 926.2141; found: 926.2108. Elemental analysis for C₄₅H₄₉F₃N₃O₆P₂PdS₂ (0.4 ^tBuCN): calc (%) C 50.47; H 4.65; N 4.01; found C 50.31; H 4.60; N 3.91.

[Pd(L^{Ph})(CN^{Bu})₂](OTf)₂ **3b**: A solution of **1b** (34.6 mg, 0.047 mmol) in CH₂Cl₂ (1.5 mL) was added to AgOTf (24.2 mg, 0.094 mmol). Upon stirring the yellow solution turned turbid after 10 minutes and a gray precipitate appeared. The stirring was stopped after 1h30, the gray precipitate was filtered through a PTFE filter. A solution of tertbutyl isocyanide (200 μL, 0.47 M solution of ^tBuNC in CH₂Cl₂) was added to the orange filtrate and the solution immediately became light-yellow. After 5 minutes stirring, the solvent was evaporated under vacuum and the yellow oil was washed with Et₂O (2 x 3 mL) before being dried under vacuum to give a light-yellow powder (40.3 mg, 0.037 mmol, 78%). IR (neat, cm⁻¹): 2245, 1482, 1437, 1262, 1222, 1142, 1028, 991. ³¹P NMR (CD₂Cl₂, 121.5 MHz): δ = 13.9 (d, J_{P,P}= 39.0 Hz, PN) and 32.2 (d, J_{P,P}= 39.0 Hz, P). ¹H NMR (CD₂Cl₂, 600 MHz): δ = 7.95 (td, J_{H,H}= 11.5 Hz, J_{H,H}= 1.5 Hz, 1H, CH_{ArP2}), 7.79 (t, J_{H,H}= 14.5 Hz, 1H, CH_{ArP2}), 7.35-7.69 (m, 18H, CH_{ArP2} and CH_{PPH2}), 7.27 (d, J= 7.0 Hz, 4H, CH_{PPH2}), 7.11 (m, 3H, CH_{Ph}), 6.85 (d, J= 4.5 Hz, 2H, CH_{Ph}), 1.40 (s, 9H, CH_{CNIBu}), 1.09 (s, 9H, CH_{CNIBu}). HRMS (ESI⁺): calculated for [C₄₂H₃₈F₃N₂O₃P₂PdS]⁺ ([Pd(L^{Ph})(CN^{Bu})(OTf)]⁺): 875.1047; found: 875.1059. Elemental analysis for C₄₈H₄₇F₃N₃O₆P₂PdS₂ (0.5 ^tBuCN): calc (%) C 52.74; H 4.51; N 4.26; found C 52.90; H 4.36; N 4.42.

[Pd(L^{TMS})(CN^{Bu})₂](OTf)₂ **3c**: A solution of **1c** (16.8 mg, 0.024 mmol) in CH₂Cl₂ (1 mL) was added to AgOTf (12.2 mg, 0.048 mmol). Upon stirring the yellow solution turned turbid after 10 minutes and a gray precipitate appeared. The stirring was stopped after 20 min., the gray precipitate was filtered through a PTFE filter. A solution of tertbutyl isocyanide (100 μL, 0.47 M solution of ^tBuNC in CH₂Cl₂) was added and the solution immediately became colorless. The solvent was immediately evaporated under vacuum and the yellow oil was washed with Et₂O (2 mL) before being dried under vacuum to give a light-yellow powder (15 mg, 0.014 mmol, 57%). IR (neat, cm⁻¹): 2233, 1437, 1254, 1145, 1029. ³¹P NMR (CDCl₃, 121.5 MHz): δ = 17.8 (d, J_{P,P}= 21.0 Hz, PN) and 30.9 (d, J_{P,P}= 21.0 Hz, P). ¹H NMR (CD₂Cl₂, 300 MHz): δ = 7.90-7.82 (m, 4H, CH_{PPH2}), 7.75-7.37 (m, 18H, CH_{ArP2} and CH_{PPH2}), 7.32-7.28 (m, 2H, CH_{ArP2}), 1.65 (s, 9H, CH_{CNIBu}), 1.39 (s, 9H, CH_{CNIBu}), -0.21 (s, 9 H, CH_{TMS}). HRMS (ESI⁺): calculated for [C₃₉H₄₂F₃N₂O₃P₂PdSSi]⁺ ([Pd(L^{TMS})(CN^{Bu})(OTf)]⁺): 871.1142; found: 871.1079; calculated for [C₄₄H₅₁F₃N₃O₃P₂PdSSi]⁺ ([Pd(L^{TMS})(CN^{Bu})₂(OTf)]⁺): 954.1883; found: 954.1807. Elemental analysis for C₄₅H₅₁F₃N₃O₆P₂PdS₂Si (0.5 ^tBuCN): calc (%) C 49.78; H 4.88; N 4.28; found C 49.66; H 4.73; N 4.41.

[Pd(L^H)(CN^{Bu})₂](OTf)₂ **3d**: **1d** (40.4 mg, 0.06 mmol) is dissolved in CH₂Cl₂ (3 mL) and added to TIOtF (42.4 mg, 0.12 mmol). Upon stirring the yellow solution turned turbid after 5 minutes and a gray precipitate appeared. The stirring was stopped after 1h30 the precipitate was filtered off thanks to a PTFE filter. A solution of tertbutyl isocyanide (250 μL, 0.47 M solution of ^tBuNC in CH₂Cl₂, 0.12 mmol) was added to the orange filtrate which immediately turned colorless. After 5 minutes stirring, the solvent was evaporated under vacuum and the colorless oil was washed with Et₂O (5 mL) before being dried under vacuum to give a white powder (40.5 mg, 0.040 mmol, 66%). IR (neat, cm⁻¹): 2227, 1437, 1262, 1144, 1111, 1029. ³¹P NMR (CD₂Cl₂, 121.5 MHz): δ = 19.2 (d, J_{P,P}= 35.0 Hz) and 31.3 (d, J_{P,P}= 35.0 Hz); ¹H NMR (CD₂Cl₂, 300 MHz): δ = 7.81 (m, 2H, CH_{ArP2}), 7.62 (m, 4H, CH_{PPH2}), 7.41 (m, 18H, CH_{ArP2} and CH_{PPH2}), 1.40 (s, 9H, CH_{CNIBu}), 1.08 (s, 9H, CH_{CNIBu}). HRMS (ESI⁺): calculated for [C₄₁H₄₃F₃N₃O₃P₂PdS]⁺ ([Pd(L^H)(CN^{Bu})₂(OTf)]⁺): 882.1482; found: 882.1492.

Supporting Information

Detailed X-ray data for L^{Ph}, **1a-d**, and **2a-d**, NMR and IR spectra as well as DFT Optimized geometries and NPA charges for I-IIIa-d.

Acknowledgements

The authors thank the Centre National de la Recherche Scientifique (CNRS), Ecole polytechnique for financial support, and Dr. S. Bourcier for mass spectrometry measurements. ANR is acknowledged for the funding of the LYMACATO project (ANR-21-CE07-0026-01), and the GDR phosphore for gathering the

community of P-chemists in France. Colleagues within this network are thanked for their help in the NMR characterization when this was not anymore possible in LCM: Dr. A. Normand and the Platform of ICMUB (Dijon), as well as Drs J.-F. Gaillard and F. Giraud at ICSN. A. M. thank GENCI and Explor computing centers for computational resources as well as ANR and CGI for their financial support of this work through Labex SEAM ANR 11 LABEX 086, ANR 11 IDEX 05 02 and the IdEx "Université Paris 2019" ANR-18-IDEX-0001.

Keywords: iminophosphorane • N,P ligand • Substituent effects • isocyanide • palladium

[1] H. Staudinger, J. Meyer, *Helv. Chim. Acta* **1919**, *2*, 635-646.

[2] a) A. W. Johnson, in *Ylides and Imines of Phosphorus*; Johnson (Ed.: A. W. Johnson), John Wiley & Sons, New York, **1993**; b) M. Köhn, R. Breinbauer, *Angew. Chem. Int. Ed.* **2004**, *43*, 3106-3116; c) H. Tanimoto, K. Kakiuchi, *Nat. Prod. Commun.* **2013**, *8*, 1021-1034; d) C. Bednarek, I. Wehl, N. Jung, U. Schepers, S. Bräse, *Chem. Rev.* **2020**, *120*, 4301-4354.

[3] a) M. Formica, D. Rozsar, G. Su, A. J. M. Farley, D. J. Dixon, **2020**, *53*, 2235-2247; b) H. Krawczyk, M. Dziegielewski, D. Deredas, A. Albrecht, Ł. Albrecht, *Chem. Eur. J.* **2015**, *21*, 10268-10277.

[4] R. Schwesinger, H. Schlemper, *Angew. Chem. Int. Ed.* **1987**, *26*, 1167-1169.

[5] See for examples a) J. J. Daly, *J. Chem. Soc.* **1964**, 3799-3810; b) E. Bohm, K. Dehnicke, J. Beck, W. Hiller, J. Strahle, A. Maurer, D. Fenske, *Z. Naturforsch., B* **1988**, *43*, 1-5; c) M. H. Holthausen, I. Mallov, D. W. Stephan, *Dalton Trans.* **2014**, *43*, 15201-15211.

[6] S. E. Garcia-Garrido, A. Presa Soto, J. García-Álvarez, in *Advances in Organometallic Chemistry, Vol. 77* (Ed.: P. J. Pérez), Academic Press, **2022**, pp. 105-168.

[7] a) M. Fukui, K. Itoh, Y. Ishii, *Bull. Chem. Soc. Jpn* **1975**, *48*, 2044-2046; b) E. W. Abel, S. A. Mucklejohn, *Inorg. Chim. Acta* **1979**, *37*, 107-111; c) A. Maurer, D. Fenske, J. Beck, J. Strähle, E. Böhm, K. Dehnicke, **1988**, *43*, 5-11; d) P. Imhoff, C. J. Elsevier, *J. Organomet. Chem.* **1989**, *361*, C61-C65; e) V. Cadierno, P. Crochet, J. Díez, J. García-Alvarez, S. E. Garcia-Garrido, S. Garcia-Granda, J. Gimeno, M. A. Rodriguez, *Dalton Trans.* **2003**, 3240-3249; f) V. Cadierno, P. Crochet, J. Díez, J. García-Alvarez, S. E. Garcia-Garrido, J. Gimeno, S. Garcia-Granda, M. A. Rodriguez, *Inorg. Chem.* **2003**, *42*, 3293-3307; g) T. Cheisson, A. Auffrant, *Dalton Trans.* **2014**, *43*, 13399-13409; h) T. Cheisson, A. Auffrant, G. Nocton, *Organometallics* **2015**, *34*, 5470-5478.

[8] a) K. Dehnicke, M. Krieger, W. Massa, *Coord. Chem. Rev.* **1999**, *182*, 19-65; b) T. Tannoux, A. Auffrant, *Coord. Chem. Rev.* **2023**, *474*, 214845.

[9] T. Cheisson, L. Ricard, F. W. Heinemann, K. Meyer, A. Auffrant, G. Nocton, *Inorg. Chem.* **2018**, *57*, 9230-9240.

[10] J. García-Álvarez, S. E. Garcia-Garrido, V. Cadierno, *J. Organomet. Chem.* **2014**, *751*, 792-808.

[11] I. Popovici, C. Barthes, T. Tannoux, C. Duhayon, N. Casaretto, A. Monari, A. Auffrant, Y. Canac, *Inorg. Chem.* **2023**, *62*, 2376-2388.

[12] L. Horner, H. Oediger, *Liebigs Ann.* **1959**, *627*, 142-162.

[13] A. Buchard, A. Auffrant, C. Klemps, L. Vu-Do, L. Boubekeur, X. F. Le Goff, P. Le Floch, *Chem. Commun.* **2007**, 1502-1504.

[14] a) D. J. Law, G. Bigam, R. G. Cavell, *Can. J. Chem.* **1995**, *73*, 635-642; b) R. W. Reed, B. Santarsiero, R. G. Cavell, *Inorg. Chem.* **1996**, *35*, 4292-4300.

[15] A. Steiner, D. Stalke, *Angew. Chem. Int. Ed. Engl.* **1995**, *34*, 1752-1755.

[16] See for examples of coordination of iminophosphorane ligands with the same Pd precursor a) M. J. Sgro, D. W. Stephan, *Dalton Trans.* **2011**, *40*, 2419-2421; b) J. García-Álvarez, J. Díez, C. Vidal, *Green Chem.* **2012**, *14*, 3190-3196; c) M. Frik, J. Jimenez, V. Vasilevski, M. Carreira, A. de Almeida, E. Gascon, F. Benoit, M. Sanau, A. Casini, M. Contel, *Inorg. Chem. From.* **2014**, *1*, 231-241; d) T. Cheisson, A. Auffrant, *Dalton Trans.* **2016**, *45*, 2069-2078.

[17] B. J. Coe, S. J. Glenwright, *Coord. Chem. Rev.* **2000**, *203*, 5-80.

[18] a) E. O'Grady, N. Kaltsoyannis, *J. Chem. Soc., Dalton Trans.* **2002**, 1233-1239; b) H. S. La Pierre, K. Meyer, *Inorg. Chem.* **2013**, *52*, 529-539; c) M. Gregson, E. Lu, D. P. Mills, F. Tuna, E. J. L. McInnes, C. Hennig, A. C. Scheinost, J. McMaster, W. Lewis, A. J. Blake, A. Kerridge, S. T. Liddle, *Nat. Commun.* **2017**, *8*, 14137.

[19] a) T. Andruniow, J. Kuta, M. Z. Zgierski, P. M. Kozłowski, *Chem. Phys. Lett.* **2005**, *410*, 410-416; b) M. V. Vollmer, J. Xie, C. C. Lu, *J. Am. Chem. Soc.* **2017**, *139*, 6570-6573.

[20] a) K. V. Katti, R. G. Cavell, R. J. Batchelor, F. W. B. Einstein, *Inorg. Chem.* **1990**, *29*, 808-814; b) M. S. Balakrishna, B. D. Santarsiero, R. G. Cavell, *Inorg. Chem.* **1994**, *33*, 3079-3084; c) C.-Y. Liu, D.-Y. Chen, M.-C. Cheng, S.-M. Peng, S.-T. Liu, *Organometallics* **1995**, *14*, 1983-1991; d) P. Molina, A. Arques, A. García, M. C. R. de Arellano, *Tetrahedron Lett.* **1997**, *38*, 7613-7616; e) P. Molina, A. Arques, A. García, M. C. Ramírez de Arellano, *Eur. J. Inorg. Chem.* **1998**, *1998*, 1359-1368; f) R. S. Pandurangi, K. V. Katti, D. Stillwell, C. L. Barnes, *J. Am. Chem. Soc.* **1998**, *120*, 11364-11373; g) A. Arques, P. Molina, D. Auñón, M. a. J. Vilaplana, M. D. Velasco, F. Martínez, D. Bautista, F. J. Lahoz, *J. Organomet. Chem.* **2000**, *598*, 329-338; h) M. Alajarín, C. López-Leonardo, P. Llamas-Lorente, D. Bautista, P. G. Jones, *Dalton Trans.* **2003**, 426-434; i) L. Boubekeur, L. Ricard, N. Mézailles, P. Le Floch, *Organometallics* **2005**, *24*, 1065-1074; j) L. Boubekeur, L. Ricard, N. Mézailles, M. Demange, A. Auffrant, P. Le Floch, *Organometallics* **2006**, *25*, 3091-3094; k) V. Cadierno, J. Díez, J. García-Álvarez, J. Gimeno, N. Nebra, J. Rubio-García, *Dalton Trans.* **2006**, 5593-5604; l) P. Crujeiras, J. L. Rodríguez-Rey, A. Sousa-Pedrares, *Eur. J. Inorg. Chem.* **2017**, *2017*, 4653-4667; m) J. L. Rodríguez-Rey, D. Esteban-Gómez, C. Platas-Iglesias, A. Sousa-Pedrares, *Dalton Trans.* **2019**, *48*, 486-503.

[21] T. Tannoux, L. Mazaud, T. Cheisson, N. Casaretto, A. Auffrant, *Dalton Trans.* **2023**, 12010-12019.

[22] G. Sheldrick, *Acta Crystallogr. A* **2015**, *71*, 3-8.

[23] O. V. Dolomanov, L. J. Bourhis, R. J. Gildea, J. A. K. Howard, H. Puschmann, *J. Appl. Crystallogr.* **2009**, *42*, 339-341.

[24] G. Sheldrick, *Acta Crystallogr. C* **2015**, *71*, 3-8.

[25] L. J. Farrugia, Department of Chemistry, University of Glasgow, **2001**.

[26] F. Neese, in *WIREs Computational Molecular Science, Vol. 8*, John Wiley & Sons, Ltd, **2018**, p. e1327.

[27] A. D. Becke, *J. Chem. Phys.* **1993**, *98*, 5648-5652.

[28] S. Grimme, J. Antony, S. Ehrlich, H. Krieg, *J. Chem. Phys.* **2010**, *132*, 154104.

[29] F. Weigend, R. Ahlrichs, *Phys. Chem. Chem. Phys.* **2005**, *7*, 3297-3305.

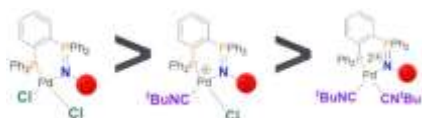
[30] J. Tomasi, B. Mennucci, R. Cammi, *Chem. Rev.* **2005**, *105*, 2999-3094.

[31] A. V. Titov, I. S. Ufimtsev, N. Luehr, T. J. Martinez, *J. Chem. Theory Comput.* **2013**, *9*, 213-221.

[32] E. D. Glendening, C. R. Landis, F. Weinhold, *J. Comput. Chem.* **2013**, *34*, 1429-1437.

[33] S. Chiodo, N. Russo, E. Sicilia, *J. Chem. Phys.* **2006**, *125*, 104107.

Entry for the Table of Contents



STABILITY



The consequences of varying the substituent of the N atom in bidentate (P,N) ligand was studied experimentally and theoretically within 3 series of palladium(II) complexes featuring also chlorides and/or isocyanides. The alkyl substituted complexes exhibit the higher stability while the H and trimethylsilyl containing counterparts were the most sensitive. For the latter, charge differences within the complexes were shown.